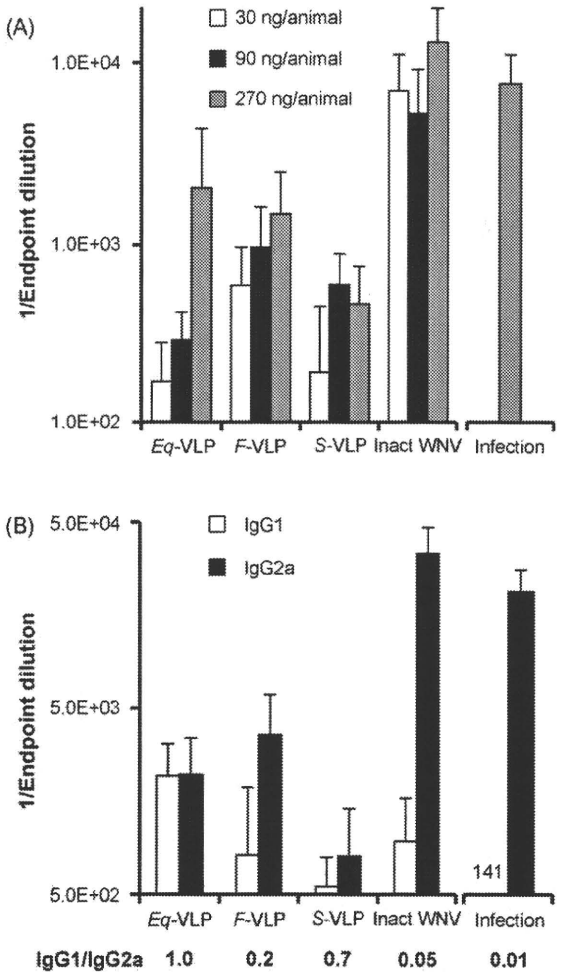

Fig. 6. WNV-specific IgG ELISA endpoint titers in mice immunized with VLPs. (A) Mice were immunized as in Table 1 and total IgG antibody titers in sera were determined by ELISA on plates coated with formalin-inactivated WNV. IgG titers in mice survived WNV infection were also shown. The cutoff values were calculated from the O.D. values of the PBS (−)-injected mouse sera. The results show the means and standard deviations. (B) Titers of IgG1 and IgG2a subclasses in mice immunized with 270 ng of VLPs were determined as in (A).

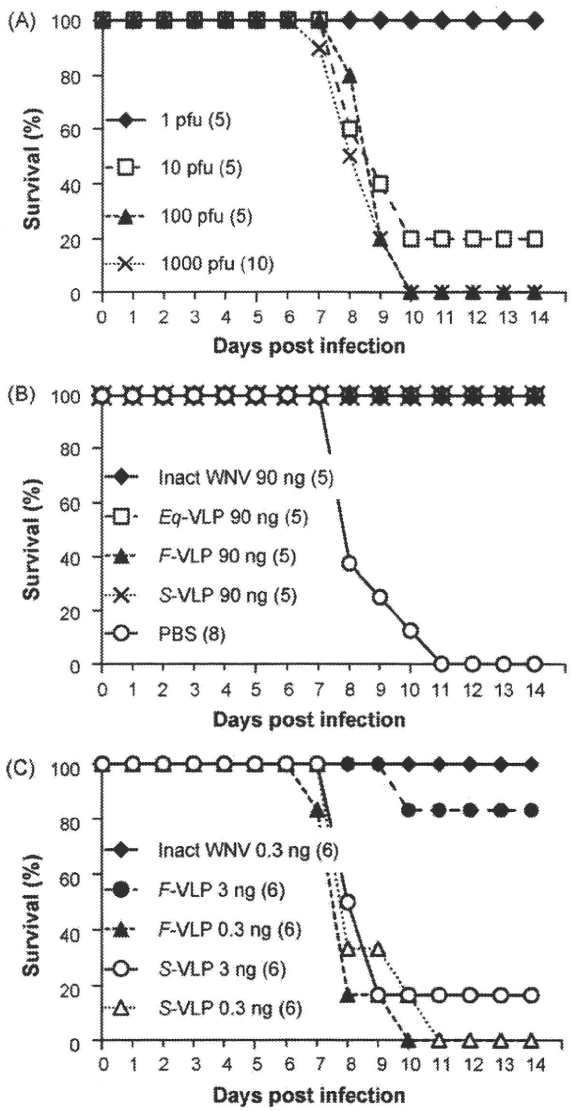

Fig. 7. Protective efficacy of VLPs against lethal WNV challenge. (A) Naïve C3H/HeN mice (6-week old) were intraperitoneally infected with 1, 10^1, 10^2 and 10^3 pfu of the WNV NY-99 strain and observed for 14 days. (B) Groups of C3H/HeN mice (4-week old) were vaccinated twice with a high dose (90 ng) of VLPs and intraperitoneally challenged with 10^3 pfu of WNV at 1 week post-vaccination. (C) Mice were vaccinated with low doses (3 and 0.3 ng) of VLPs and challenged with WNV as in (B). The number of mice in each group is shown in the parentheses of each graph.

the three types of VLPs as in immunization experiments and were challenged at the age of 6 weeks with 10^3 pfu of WNV. Fig. 7B shows that a high dose (90 ng) of the VLP antigens rendered mice protective against WNV and mice vaccinated with *Eq*-VLPs, *F*-VLPs and *S*-VLPs survived 100% without detectable clinical signs. In order to examine whether *F*-VLPs and *S*-VLPs are different in their ability to develop protective immunity, low doses (3 and 0.3 ng) of *F*-VLPs and *S*-VLPs were inoculated into groups of six mice. These mice were challenged with 10^3 pfu of WNV and observed daily for 2 weeks (Fig. 7C). Five out of six (83%) mice immunized with 3 ng of *F*-VLPs were survived from the lethal dose of WNV infection. In contrast to *F*-VLPs, the same dose of *S*-VLPs saved only one (17%) mouse. Mice receiving a much lower dose (0.3 ng) of *F*-VLPs and *S*-VLPs similarly showed the clinical course of infection and died 100%, although all the mice survived with 0.3 ng of inactivated WNV. These results suggest that *F*-VLPs are superior to *S*-VLPs in immunogenicity and protective efficacy against WNV as well.

4. Discussion

We have successfully established CHO #22.6S cells that continuously express the WNV prM–E gene and stably produce WNV VLPs in serum-free cultures. In this study, two distinct types of VLPs were found to be secreted from the established cells; larger (40–50 nm in diameter) *F*-VLPs and smaller (20–30 nm in diameter) *S*-VLPs, which could be separated by velocity sedimentation. So far, two distinct size classes of flaviviral VLPs were only observed by the expression of the tick-borne encephalitis virus (TBEV) prM–E gene in transfected COS-1 cells [33]. Previous studies on the flavivirus morphogenesis argued that packaging of the viral RNA into a core composed of the C proteins was a prerequisite to form particles in the virion sizes [34]. However, our *F*-VLPs of WNV and their large RSPs of TBEV are similar in size to the original whole viruses without the C proteins. Both large VLPs and RSPs were distinguished from small ones by velocity sedimentation in gradients prepared with lower concentrations of sucrose, and were fractionated at similar migration rates. The mature M proteins were a major component of the large VLP/RSP particles, when generated from the wild-type prM–E genes of WNV and TBEV. However, RSPs with the immature prM protein were produced in a large size from a TBEV prM–E gene derivative by a mutation at the furin cleavage site. On the other

hand, *S*-VLPs and small RSPs have similar appearances to prM/M–E VLPs of other flaviviruses [10–12]. It is known that flavivirus-infected cells produce not only infectious virus particles but smaller noninfectious particles called slowly sedimenting hemagglutinin (SHA). SHAs are separated from the virions by sucrose gradient centrifugation and show similar sedimenting profiles to prM/M–E VLPs [15,35]. Taken together, *F*-VLPs and *S*-VLPs may be analogous to infectious virions and SHAs, respectively.

Interestingly, the processed mature M and unprocessed immature prM proteins were major and minor, respectively, in larger *F*-VLPs; reversely in smaller *S*-VLPs, however, the M and prM proteins were minor and major, respectively (Fig. 5E). This result may suggest some effects of proteolytic processing of prM into M on VLP sizes. The prM and E proteins of flaviviruses are thought to associate into heterodimers, to assemble into immature particles and to bud into the lumen of the ER in small SHA or VLP size. During traffic through the secretory pathway, a significant portion of prM is cleaved by host furin protease in the trans-Golgi to form the M protein. Recent X-ray crystallography of the E proteins and cryo-electron microscopy of the flavivirus particles have proposed a model where trimeric prM/E heterodimers form progenitor particles and processing of prM into M allows to generate E homodimers in association with mature M and to form infectious viruses with diameters of about 50 nm [7,8]. Similarly to the model, the prM cleavage of smaller VLPs in the Golgi might induce the conformational rearrangement of the prM/E heterodimers to the E homodimers associated with processed M and make the small particles appear larger, although prM-unprocessed particles preserve small VLP size. In addition, several papers suggest the processing effects. The disruption of cellular furin protease or the improper digestion by host signalase decreases viral infectivity and increases the production of small, noninfectious SHAs [36,37]. The proportion of the immature prM proteins to total prM/M proteins is high in SHAs and that of the mature M proteins is high in the whole virions [35].

Glycosylation of the structural proteins is a constitutive factor that affects flavivirus assembly [9]. Thus, the ratios of large and small VLPs are possibly regulated by the modification with sugar chains. The sizes of our VLPs are, however, unlikely to depend on the glycosylation status, since the E proteins of WNV VLPs were resistant to Endo H_f digestion as WNV virions. In case of TBEV RSPs, on the other hand, the E glycoproteins of the larger particles were slightly more sensitive to Endo H_f glycosidase than those of the smaller particles [33]. Although subtle differences in the structural environment of the sugar chains are discussed for TBEV RSPs, subtle delays in the processing of the prM–E polyprotein may happen to our *F*- and *S*-VLPs in intracellular transport pathways and alter the relative release rate of large and small VLPs.

If the processed M and unprocessed prM proteins could differentially modulate the organization of the E proteins on large and small VLPs, it is possible that *F*- and *S*-VLPs are different in their antigenic forms. Thus, it is important to address antibody responses induced with *F*-VLPs and *S*-VLPs. Our results show that *F*-VLPs were superior to other forms of VLPs. NTAb titers against WNV increased with immunizing doses of *F*-VLPs. However, small *S*-VLPs and shrunken *Eq*-VLPs induced lower levels of NTAbs at higher immunizing doses. Furthermore, IgG2a-dominant antibody responses were induced by *F*-VLPs and the whole virion-derived antigens, such as formalin-inactivated and infectious viruses, but not by *S*-VLPs and *Eq*-VLPs. These data are consistent with the previous studies revealing that the recombinant TBEV antigens forming subviral particles and the attenuated replicons could induce high NTAb titers with IgG2a dominance [38–40]. Therefore, the E proteins of *F*-VLPs appear to be rearranged upon prM cleavage to more immunogenic conformations.

In contrast to *F*-VLPs, *S*-VLPs were a poorer immunogen. Levels of IgG antibodies were low and not dominant to the IgG2a subclass. NTAb titers unexpectedly decreased with increasing *S*-VLP dose. The *S*-VLP preparation contained a considerable amount of CHO-S-derived cellular debris. Therefore, a possibility is that the contaminating cellular proteins from CHO lines expressing prM–E may be cross-reactive and inhibit immunogenic stimulus on B-cell clones at high doses of the *S*-VLP preparation. However, the shrunken *Eq*-VLP preparation in which the cellular microsomal vesicles or debris were rather a low amount, induced antibody responses as the *S*-VLP preparation did in terms of NTAb titers and the IgG subclass distribution. Furthermore, *S*-VLPs were observed as clearly distinct particles from *F*-VLPs in both size and appearance. Therefore, differences in the morphological forms between *F*-VLPs and *S*-VLPs are likely to reflect their immunogenicity to induce protective antibody responses.

All types of our VLPs, however, completely protected mice against WNV infection when a sufficient dose (90 ng per animal) was used for immunization. The critical roles of antibodies have been described to protect against WNV-induced mortality [17,18] and the high dose (90 ng) of VLPs all induced substantial levels of NTAb titers. In contrast, a low dose (3 ng) of *F*-VLPs showed apparently higher protective efficacy against WNV than *S*-VLPs. In addition to NTAbs, *F*-VLPs possessed antigenicity favorable to IgG2a-dominant antibody responses, which are promoted by T-helper 1 lymphocytes that are responsible for inducing cell-mediated immune responses [38,39,41]. Besides NTAbs, cytotoxic T-lymphocyte responses are also known to have an important function in flavivirus clearance [42]. Thus, the different morphological forms of VLPs appear to affect the host defense against WNV pathogenesis and large *F*-VLPs are able to induce better protective immunity than small *S*-VLPs.

In summary, we have succeeded in separating immunogenic *F*-VLPs from *S*-VLPs and host cell-derived impurities, and suggested that large *F*-VLPs produced in serum-free cultures of #22.6S cell clones are a promising candidate as a second-generation WNV vaccine. To accomplish it, the optimization of sucrose density gradient centrifugation was needed for purification of the large, mature *F*-VLPs without shrinkage of the particles. The procedures described here would be applicable for other flavivirus VLPs as well as the viral replicon particles and attenuated virions [20–23] to refining their immunogenicity as flavivirus vaccines.

Acknowledgements

This work was supported in part by research grants from the Ministry of Health, Labor, and Welfare, and from the Japanese Health Sciences Foundation (A. Kojima).

References

[1] Dauphin G, Zientara S. West Nile virus: recent trends in diagnosis and vaccine development. Vaccine 2007;25(July (30)):5563–76.
[2] Iwamoto M, Jernigan DB, Guasch A, Trepka MJ, Blackmore CG, Hellinger WC, et al. Transmission of West Nile virus from an organ donor to four transplant recipients. N Engl J Med 2003;348(May (22)):2196–203.
[3] Pealer LN, Marfin AA, Petersen LR, Lanciotti RS, Page PL, Stramer SL, et al. Transmission of West Nile virus through blood transfusion in the United States in 2002. N Engl J Med 2003;349(September (13)):1236–45.
[4] Kuhn RJ, Zhang W, Rossmann MG, Pletnev SV, Corver J, Lenches E, et al. Structure of dengue virus: implications for flavivirus organization, maturation, and fusion. Cell 2002;108(March (5)):717–25.
[5] Mukhopadhyay S, Kim BS, Chipman PR, Rossmann MG, Kuhn RJ. Structure of West Nile virus. Science 2003;302(October (5643)):248.
[6] Lorenz IC, Allison SL, Heinz FX, Helenius A. Folding and dimerization of tick-borne encephalitis virus envelope proteins prM and E in the endoplasmic reticulum. J Virol 2002;76(June (11)):5480–91.
[7] Li L, Lok SM, Yu IM, Zhang Y, Kuhn RJ, Chen J, et al. The flavivirus precursor membrane-envelope protein complex: structure and maturation. Science 2008;319(March (5871)):1830–4.

[8] Zhang Y, Kaufmann B, Chipman PR, Kuhn RJ, Rossmann MG. Structure of immature West Nile virus. J Virol 2007;81(June (11)):6141–5.
[9] Hanna SL, Pierson TC, Sanchez MD, Ahmed AA, Murtadha MM, Doms RW. N-linked glycosylation of west nile virus envelope proteins influences particle assembly and infectivity. J Virol 2005;79(November (21)):13262–74.
[10] Konishi E, Pincus S, Paoletti E, Shope RE, Burrage T, Mason PW. Mice immunized with a subviral particle containing the Japanese encephalitis virus prM/M and E proteins are protected from lethal JEV infection. Virology 1992;188(June (2)):714–20.
[11] Mutoh E, Ishikawa T, Takamizawa A, Kurata T, Sata T, Kojima A. Japanese encephalitis subunit vaccine composed of virus-like envelope antigen particles purified from serum-free medium of a high-producer J12#26 cell clone. Vaccine 2004;22(June (20)):2599–608.
[12] Schalich J, Allison SL, Stiasny K, Mandl CW, Kunz C, Heinz FX. Recombinant subviral particles from tick-borne encephalitis virus are fusogenic and provide a model system for studying flavivirus envelope glycoprotein functions. J Virol 1996;70(July (7)):4549–57.
[13] Takahashi H, Ohtaki N, Maeda-Sato M, Tanaka M, Tanaka K, Sawa H, et al. Effects of the number of amino acid residues in the signal segment upstream or downstream of the NS2B-3 cleavage site on production and secretion of prM/M–E virus-like particles of West Nile virus. Microbes Infect 2009;11(November (13)):1019–28.
[14] Ferlenghi I, Clarke M, Ruttan T, Allison SL, Schalich J, Heinz FX, et al. Molecular organization of a recombinant subviral particle from tick-borne encephalitis virus. Mol Cell 2001;7(March (3)):593–602.
[15] Mason PW, Pincus S, Fournier MJ, Mason TL, Shope RE, Paoletti E. Japanese encephalitis virus-vaccinia recombinants produce particulate forms of the structural membrane proteins and induce high levels of protection against lethal JEV infection. Virology 1991;180(January (1)):294–305.
[16] Chiba N, Osada M, Komoro K, Mizutani T, Kariwa H, Takashima I. Protection against tick-borne encephalitis virus isolated in Japan by active and passive immunization. Vaccine 1999;17(March (11–12)):1532–9.
[17] Diamond MS, Shrestha B, Marri A, Mahan D, Engle M. B cells and antibody play critical roles in the immediate defense of disseminated infection by West Nile encephalitis virus. J Virol 2003;77(February (4)):2578–86.
[18] Engle MJ, Diamond MS. Antibody prophylaxis and therapy against West Nile virus infection in wild-type and immunodeficient mice. J Virol 2003;77(December (24)):12941–9.
[19] Oya A. Japanese encephalitis vaccine. Acta Paediatr Jpn 1988;30(April (2)):175–84.
[20] Widman DG, Ishikawa T, Fayzulin R, Bourne N, Mason PW. Construction and characterization of a second-generation pseudoinfectious West Nile virus vaccine propagated using a new cultivation system. Vaccine 2008;26(May (22)):2762–71.
[21] Yu L, Robert Putnak J, Pletnev AG, Markoff L. Attenuated West Nile viruses bearing 3'SL and envelope gene substitution mutations. Vaccine 2008;26(November (47)):5981–8.
[22] Monath TP, Liu J, Kanesa-Thasan N, Myers GA, Nichols R, Deary A, et al. A live, attenuated recombinant West Nile virus vaccine. Proc Natl Acad Sci U S A 2006;103(April (17)):6694–9.
[23] Pletnev AG, Swayne DE, Speicher J, Rumyantsev AA, Murphy BR. Chimeric West Nile/dengue virus vaccine candidate: preclinical evaluation in mice, geese and monkeys for safety and immunogenicity. Vaccine 2006;24(September (40–41)):6392–404.
[24] Despres P, Combredet C, Frenkiel MP, Lorin C, Brahic M, Tangy F. Live measles vaccine expressing the secreted form of the West Nile virus envelope glycoprotein protects against West Nile virus encephalitis. J Infect Dis 2005;191(January (2)):207–14.
[25] Martin JE, Pierson TC, Hubka S, Rucker S, Gordon IJ, Enama ME, et al. A West Nile virus DNA vaccine induces neutralizing antibody in healthy adults during a phase 1 clinical trial. J Infect Dis 2007;196(December (12)):1732–40.
[26] Lim CK, Takasaki T, Kotaki A, Kurane I. Vero cell-derived inactivated West Nile (WN) vaccine induces protective immunity against lethal WN virus infection in mice and shows a facilitated neutralizing antibody response in mice previously immunized with Japanese encephalitis vaccine. Virology 2008;374(April (1)):60–70.
[27] Bonafe N, Rininger JA, Chubet RG, Foellmer HG, Fader S, Anderson JF, et al. A recombinant West Nile virus envelope protein vaccine candidate produced in *Spodoptera frugiperda* expresSF+ cells. Vaccine 2009;27(January (2)):213–22.
[28] Lieberman MM, Clements DE, Ogata S, Wang G, Corpuz G, Wong T, et al. Preparation and immunogenic properties of a recombinant West Nile subunit vaccine. Vaccine 2007;25(January (3)):414–23.
[29] Martina BE, Koraka P, van den Doel P, van Amerongen G, Rimmelzwaan GF, Osterhaus AD. Immunization with West Nile virus envelope domain III protects mice against lethal infection with homologous and heterologous virus. Vaccine 2008;26(January (2)):153–7.
[30] Gehrke R, Ecker M, Aberle SW, Allison SL, Heinz FX, Mandl CW. Incorporation of tick-borne encephalitis virus replicons into virus-like particles by a packaging cell line. J Virol 2003;77(August (16)):8924–33.
[31] Konishi E, Fujii A, Mason PW. Generation and characterization of a mammalian cell line continuously expressing Japanese encephalitis virus subviral particles. J Virol 2001;75(March (5)):2204–12.
[32] Kojima A, Yasuda A, Asanuma H, Ishikawa T, Takamizawa A, Yasui K, et al. Stable high-producer cell clone expressing virus-like particles of the Japanese encephalitis virus e protein for a second-generation subunit vaccine. J Virol 2003;77(August (16)):8745–55.
[33] Allison SL, Tao YJ, O'Riordain G, Mandl CW, Harrison SC, Heinz FX. Two distinct size classes of immature and mature subviral particles from tick-borne encephalitis virus. J Virol 2003;77(November (21)):11357–66.
[34] Patkar CG, Jones CT, Chang YH, Warrier R, Kuhn RJ. Functional requirements of the yellow fever virus capsid protein. J Virol 2007;81(June (12)):6471–81.
[35] Ishikawa T, Konishi E. Mosquito cells infected with Japanese encephalitis virus release slowly-sedimenting hemagglutinin particles in association with intracellular formation of smooth membrane structures. Microbiol Immunol 2006;50(3):211–23.
[36] Junjhon J, Lausumpao M, Supasa S, Noisakran S, Songjaeng A, Saraithong P, et al. Differential modulation of prM cleavage, extracellular particle distribution, and virus infectivity by conserved residues at nonfurin consensus positions of the dengue virus pr-M junction. J Virol 2008;82(November (21)):10776–91.
[37] Lobigs M, Lee E. Inefficient signalase cleavage promotes efficient nucleocapsid incorporation into budding flavivirus membranes. J Virol 2004;78(January (1)):178–86.
[38] Aberle JH, Aberle SW, Allison SL, Stiasny K, Ecker M, Mandl CW, et al. A DNA immunization model study with constructs expressing the tick-borne encephalitis virus envelope protein E in different physical forms. J Immunol 1999;163(December (12)):6756–61.
[39] Aberle JH, Aberle SW, Kofler RM, Mandl CW. Humoral and cellular immune response to RNA immunization with flavivirus replicons derived from tick-borne encephalitis virus. J Virol 2005;79(December (24)):15107–13.
[40] Heinz FX, Allison SL, Stiasny K, Schalich J, Holzmann H, Mandl CW, et al. Recombinant and virion-derived soluble and particulate immunogens for vaccination against tick-borne encephalitis. Vaccine 1995;13(December (17)):1636–42.
[41] Finkelman FD, Holmes J, Katona IM, Urban Jr JF, Beckmann MP, Park LS, et al. Lymphokine control of in vivo immunoglobulin isotype selection. Annu Rev Immunol 1990;8:303–33.
[42] Shrestha B, Diamond MS. Role of CD8+ T cells in control of West Nile virus infection. J Virol 2004;78(August (15)):8312–21.

Bioorganic & Medicinal Chemistry Letters 20 (2010) 354–358

Contents lists available at ScienceDirect

Bioorganic & Medicinal Chemistry Letters

journal homepage: www.elsevier.com/locate/bmcl

CD4 mimics targeting the mechanism of HIV entry

Yuko Yamada [a], Chihiro Ochiai [a], Kazuhisa Yoshimura [b], Tomohiro Tanaka [a], Nami Ohashi [a], Tetsuo Narumi [a], Wataru Nomura [a], Shigeyoshi Harada [b], Shuzo Matsushita [b], Hirokazu Tamamura [a,*]

[a] Institute of Biomaterials and Bioengineering, Tokyo Medical and Dental University, Chiyoda-ku, Tokyo 101-0062, Japan
[b] Center for AIDS Research, Kumamoto University, Kumamoto 860-0811, Japan

ARTICLE INFO

Article history:
Received 19 September 2009
Revised 20 October 2009
Accepted 22 October 2009
Available online 4 November 2009

Keywords:
CD4 mimic
HIV entry
Synergistic effect
CXCR4

ABSTRACT

A structure–activity relationship study was conducted of several CD4 mimicking small molecules which block the interaction between HIV-1 gp120 and CD4. These CD4 mimics induce a conformational change in gp120, exposing its co-receptor-binding site. This induces a highly synergistic interaction in the use in combination with a co-receptor CXCR4 antagonist and reveals a pronounced effect on the dynamic supramolecular mechanism of HIV-1 entry.

Recently, remarkable success has attended the clinical treatment of HIV-infected and AIDS patients, with 'highly active antiretroviral therapy (HAART)'. This approach involves a combination of two or three agents from two categories: reverse transcriptase inhibitors and protease inhibitors.[1] In addition, the molecular mechanism involved in HIV-entry and -fusion into host cells has been described in detail.[2] The complex interactions of surface proteins on cellular and viral membranes, which are designated as a dynamic supramolecular mechanism of HIV entry, are reported to be crucial to the viral infection. In a first step, an HIV envelope protein, gp120 interacts with a cell surface protein, CD4, leading to a conformational change in gp120 followed by subsequent binding of gp120 to a co-receptor CCR5[3] or CXCR4.[4] CCR5 and CXCR4 are the major co-receptors for the entry of macrophage-tropic (R5-) and T cell line-tropic (X4-) HIV-1, respectively. The interaction of gp120 with CCR5 or CXCR4 triggers entry of another envelope protein, gp41 to the cell membrane and formation of a gp41 trimer-of-hairpins structure, which causes fusion of HIV/cell-membranes and completes the infection.

Informed by this mechanism, a fusion inhibitor, enfuvirtide (fuzeon, Trimers & Roche)[5] and a CCR5 antagonist, maraviroc (Pfizer)[6] in addition to an integrase inhibitor, raltegravir (Merck)[7] have been used clinically. However, serious problems with chemotherapy still persist, including the emergence of viral strains with multi-drug resistance (MDR), considerable adverse effects and high costs. Consequently, development of novel drugs possessing mechanisms of action different from those of the above inhibitors is currently required. We have previously developed selective CXCR4 antagonists[8] and fusion inhibitors.[9] Furthermore, *N*-(4-Bromophenyl)-*N'*-(2,2,6,6-tetramethylpiperidin-4-yl)-oxalamide (**1**) and *N*-(4-chlorophenyl)-*N'*-(2,2,6,6-tetramethylpiperidin-4-yl)-oxalamide (**2**) were previously found using chemical library screening to inhibit syncytium formation by other researchers.[10] **1** and **2** bind to gp120 with binding affinities of K_d = 2.2 μM and 3.7 μM, respectively, blocking the interaction of gp120 with CD4 in the first step of an HIV-1 entry. Thus, in the present study we focus on the development of CD4 mimics that can block the interaction between gp120 and CD4. We have investigated the effect of CD4 mimics on conformational changes of gp120 and on their use in combination use with a CXCR4 antagonist.

Initially, molecular modeling of compound **2** docked into gp120 was carried out using docking simulations performed by the FlexSIS module of SYBYL 7.1 (Tripos, St. Louis) (Fig. 1).[11] The atomic coordinates of the crystal structure of gp120 with soluble CD4 (sCD4) were retrieved from Protein Data Bank (PDB) (entry 1RZJ) (Fig. 1a) and it was observed that Phe^{43} and Arg^{59} of the CD4 have multiple contacts with Asp^{368}, Glu^{370} and Trp^{427} of gp120, which are all conserved residues. An inspection of the environment of compound **2** docked in gp120 revealed the presence of a large cavity around the *p*-position of the phenyl ring of compound **2**, which could interact with the viral surface protein gp120 (Fig. 1b and c). Several analogs of **2** with substituents on the phenyl ring were therefore synthesized.

All compounds except **12** were synthesized by previously published methods (Scheme 1).[10b,12,13] Aniline derivatives (**3**) were coupled with ethyl oxalyl chloride to yield the corresponding ethyl oxalamates **4**. Saponification of the above oxalamates to the corresponding free acids and the subsequent coupling with 4-ami-

* Corresponding author.
E-mail address: tamamura.mr@tmd.ac.jp (H. Tamamura).

0960-894X/$ - see front matter © 2009 Elsevier Ltd. All rights reserved.
doi:10.1016/j.bmcl.2009.10.098

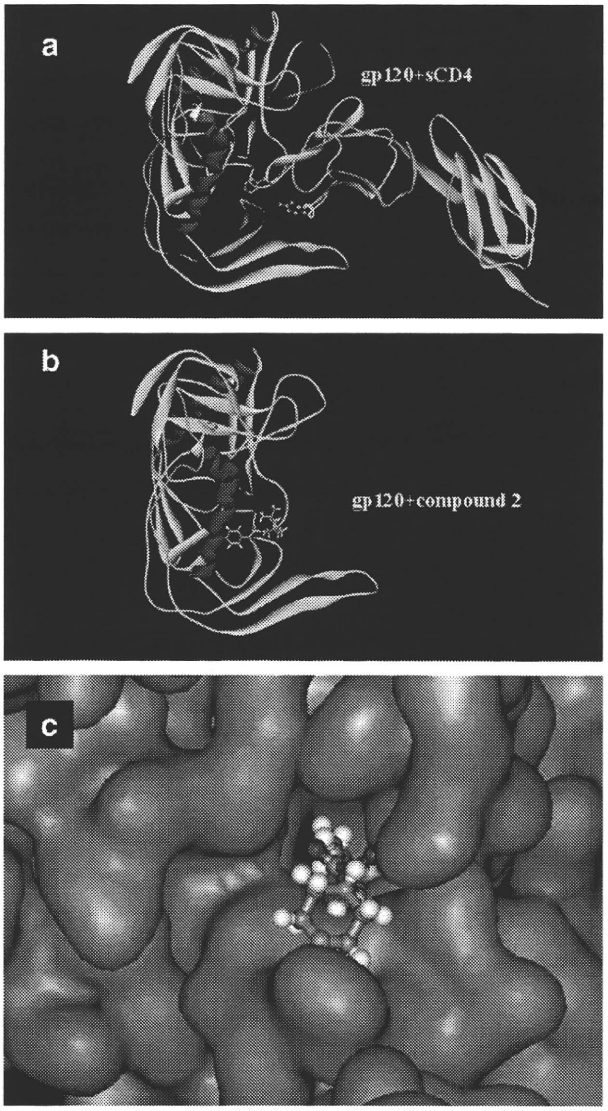

Figure 1. (a) The crystal structure of gp120 with soluble CD4 (sCD4) retrieved from the PDB (entry 1RZJ); (b) docking structure of compound **2** and gp120; (c) a focused figure of (b) shown by space-filling model.

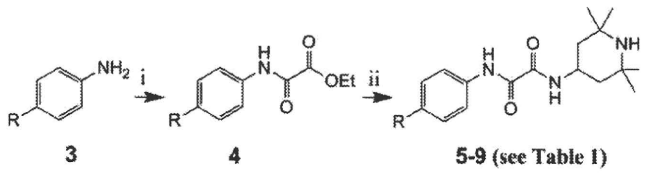

Scheme 1. Reagents and conditions: (i) ethyl oxalyl chloride, Et_3N; (ii) 1 M NaOH; 4-amino-2,2,6,6-tetramethylpiperidine, 1-(3-dimethylaminopropyl)-3-ethylcarbodiimide hydrochloride, 1-hydroxybenzotriazole, Et_3N.

no-2,2,6,6-tetramethylpiperidine using 1-ethyl-3-(3-dimethylaminopropyl)carbodiimide hydrochloride (EDC) and 1-hydroxybenzotriazole (HOBt) yielded compounds **5–9**. In the case of compound **12**, whose amide bond is not stable during the reaction of the saponification of the corresponding oxalamates, an alternative synthetic scheme was used (Scheme 2).[14] The reaction of *p*-nitroaniline (**10**) with oxalyl chloride gave the corresponding oxoacetamide **11**, which was subsequently coupled with 4-amino-2,2,6,6-tetramethylpiperidine to yield the desired compound **12**.

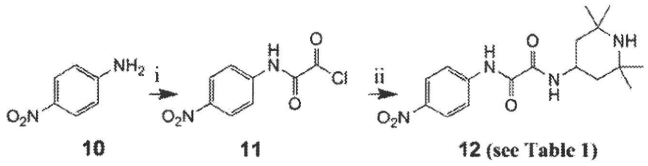

Scheme 2. Reagents and conditions: (i) oxalyl chloride, Et_3N; (ii) 4-amino-2,2,6,6-tetramethylpiperidine, Et_3N.

The anti-HIV activity of the synthetic compounds was evaluated against various viral strains including both laboratory and primary isolates (Table 1). IC_{50} values were determined by the 3-(4,5-dimethylthiazol-2-yl)-2,5-diphenyltetrazolium bromide (MTT) method[15] as the concentrations of the compounds which conferred 50% protection against HIV-1-induced cytopathogenicity in PM1/CCR5 cells. Cytotoxicity of the compounds based on the viability of mock-infected PM1/CCR5 cells was also evaluated using the MTT method. CC_{50} values were determined as the concentrations achieving 50% reduction of the viability of mock-infected cells. Compounds **1** and **2** showed potent anti-HIV activity against laboratory isolates, IIIB (X4, Sub B) and 89.6 (dual, Sub B) strains, and compound **2** also possessed potent activity against a primary isolate, an fTOI strain (R5, Sub B). All of the IC_{50} values were between 4 μM and 10 μM. Compound **1** was not tested against primary isolates. The potencies of compounds **1** and **2** are comparable to the reported binding affinities for gp120 (K_d = 2.2 and 3.7 μM, respectively).[10] Several of the new analogs of compounds **1** and **2** showed significant anti-HIV activity. Compound **5**, which has a phenyl group in place of the *p*-chlorophenyl group of compound **2**, did not show significant anti-HIV activity at concentrations below 100 μM against all strains tested except for an fTOI strain (R5, Sub B). This result suggests that a substituent at the *p*-position of the phenyl ring is critical for potent activity. Compound **6**, which has a fluorine atom at the *p*-position of the phenyl ring, showed moderate anti-HIV activity against laboratory isolates, IIIB (X4, Sub B) and 89.6 (dual, Sub B) strains (IC_{50} = 61 and 81 μM, respectively), but, at concentrations below 100 μM, failed to show significant anti-HIV activity against a primary isolate, a KYAG strain (R5, Sub B). Among halogen atoms, fluorine is less suitable than bromine or chlorine as a substituent at the *p*-position of the phenyl ring, as evidenced by compound **6**, which is 8–15-fold less potent than compounds **1** and **2** against IIIB (X4, Sub B) and 89.6 (dual, Sub B) strains. Compound **7**, which has a methyl group at the *p*-position of the phenyl ring, showed relatively more potent activity against IIIB (X4, Sub B) and 89.6 (dual, Sub B) strains (IC_{50} = 23 and 41 μM, respectively) than compound **6**. Compound **7** also showed significant anti-HIV activity against primary isolates, fTOI (R5, Sub B) and KYAG (R5, Sub B) strains (IC_{50} = 16 and 51 μM, respectively). Compound **8**, with a methoxy group at the *p*-position of the phenyl ring, did not show significant anti-HIV activity against all strains tested until a concentration of 100 μM was reached. In the biological assays, derivatives having electron-withdrawing substituents such as bromine, chlorine and fluorine at the *p*-position of the phenyl ring are relatively potent, whereas derivatives having electron-donating groups such as methoxy at this position are not potent. Furthermore, the steric effect of a substituent at the *p*-position of the phenyl ring appears to be critical to anti-HIV activity. The sum of Hammett constants (σ) of benzoic acid substituents[16] shown in Table 1 can be used to evaluate the electron-withdrawing or -donating effect of the substituents on the aromatic ring. The Taft E_s values[16a,17] were used as steric parameters for substituents at the *p*-position of the phenyl ring. The order of potency found for the halogen-containing derivatives in anti-HIV activity against laboratory isolates, IIIB (X4, Sub B) and 89.6 (dual, Sub B), is: compound **1** (R = Br) (σ = 0.23, E_s = −1.16), **2**

Table 1
Hammett constants (σ) and steric effects (E_s) of substituted aromatic rings and anti-HIV activity and cytotoxicity of synthetic compounds

Compd	R[a]	σ[b]	E_s[c]	IC_{50}[e] (μM)				CC_{50}[e] (μM)
				Lab. isolates		Primary isolates		
				IIIB (X4)	89.6 (dual)	fTOI (R5)	KYAG (R5)	
1	Br	0.23	−1.16	4	9	ND	ND	150
2	Cl	0.23	−0.97	8	10	5	>30	170
5	H	0	0	>100	>100	81	>100	350
6	F	0.06	−0.46	61	81	ND	>100	320
7	CH_3	−0.17	−1.24	23	41	16	51	210
8	OCH_3	−0.27	−0.55	>100	>100	ND	>100	340
9	CF_3	0.54	−2.40	ND	27	ND	ND	72
12	NO_2	0.78	−1.77[d]	ND	42	ND	ND	230
sCD4				0.010	0.021	0.0044	ND	ND

[a] See Schemes 1 and 2.
[b] σ = Hammett constant of a substitutent on a benzoic acid derivative.[16]
[c] E_s = steric effect of a substituent at the *para* position on the aromatic ring.[16a,17]
[d] The average value of −1.01 and −2.52, which are E_s values of the NO_2 group, −1.77, was used.
[e] Values are means of at least three experiments (ND = not determined).

(R = Cl) (σ = 0.23, E_s = −0.97), **6** (R = F) (σ = 0.06, E_s = −0.46) and **5** (R = H) (σ = 0, E_s = 0). This is the order of substituents' electron-withdrawing ability and also of their size. Methyl (σ = −0.17, E_s = −1.24) is an electron-donating group, but is almost as bulky as a bromine atom. Thus, the *p*-methyl derivative **7** has relatively potent anti-HIV activity against laboratory isolates, IIIB (X4, Sub B) and 89.6 (dual, Sub B), higher than that of compound **6** (R = F) but lower than that of compound **1** (R = Br) or **2** (R = Cl). The electron-donating ability of a methoxy group is stronger (σ = −0.27), but the bulk size is smaller (E_s = −0.55), than that of a methyl group. Thus, the *p*-methoxy derivative **8** has no significant anti-HIV activity against all strains tested at concentrations below 100 μM. Two derivatives containing bulkier and more potent electron-withdrawing substituents such as trifluoromethyl (R = CF_3) (σ = 0.54, E_s = −2.40) and nitro (R = NO_2) (σ = 0.78, E_s = −1.77) at the *p*-position of the phenyl ring were evaluated. Compounds **9** (R = CF_3) and **12** (R = NO_2) showed significant anti-HIV activity against an 89.6 (dual, Sub B) strain. These are less potent than compounds **1** and **2** and this is perhaps due to the excessive size of the substituents at the *p*-position. This suggests that a certain level of the bulk size and a potent electron-withdrawing ability of the substituents are preferable for anti-HIV activity. It is estimated that a cavity around the *p*-position of the phenyl ring of CD4 mimicking compounds would be optimally filled by bromine (E_s = −1.16) or a methyl group (E_s = −1.24) at *p*-position, and that an electron-deficient aromatic ring might interact tightly with a negatively charged group such as carboxy of Glu^{370}. In isothermal titration calorimetry (ITC) experiments reported elsewhere,[10c] compound **5** (R = H) does not have significant affinity for gp120, and compound **6** (R = F) has less potent affinity for gp120 than compound **2**, consistent with the present data. In all but one of the compounds, no significant cytotoxicity was detected (CC_{50} >150 μM, Table 1), the exception being compound **9** (R = CF_3) (CC_{50} = 72 μM). Compounds **7** and **12** have relatively low cytotoxicities, compared to compounds **1** and **2**.

Fluorescence activated cell sorting (FACS) analysis was performed[15] to investigate whether these synthetic compounds interact with gp120 inducing the conformational change necessary for the approach of an anti-envelope antibody or a co-receptor to the gp120. The profile of binding of an anti-envelope CD4-induced monoclonal antibody, 4C11, to the Env-expressing cell surface (an R5-HIV-1 strain, JR-FL,-infected PM1 cells) pretreated with the above CD4 mimic analogs was examined. Comparison of the binding of 4C11 to the cell surface was measured in terms of the mean fluorescence intensity (MFI), and is shown in Figure 2. Pretreatment of the Env-expressing cells with compound **2** (MFI = 38.42) produced a remarkable increase in binding affinity for 4C11, similar to that observed in pretreatment with sCD4 (MFI = 37.90). This is consistent with the results in the previous paper[10] where it was reported that compound **2** enhances the binding of gp120 to the 17b monoclonal antibody which recognizes the co-receptor binding site of gp120. Env-expressing cells, which were not pretreated with sCD4 or a CD4 mimic compound, did not show significant binding affinity for 4C11 (Fig. 2, blank). The increase in binding affinity for monoclonal antibodies may be due to conformational changes in gp120, which were caused by the interaction of sCD4 or a CD4 mimic with gp120. It is hypothesized that such conformational changes involve the exposure of the co-receptor binding site of gp120 (the V3 loop), which is hidden internally, since the binding of gp120 to 17b is enhanced. Compound **5**, which failed to show significant anti-HIV activity, and compounds **7**, **9** and **12**, which had significant anti-HIV activity, were assessed in the FACS analysis. The profile of the binding of 4C11 to the Env-expressing cell surface pretreated with compound **5** (MFI = 14.34) was similar to that of the blank (MFI = 11.24), suggesting that compound **5** offers no significant enhancement of binding affinity for 4C11. This result is compatible with the anti-HIV activity of compound **5**. The profile of the binding of 4C11 to the Env-expressing cell surface pretreated with compound **7** (MFI = 38.33) was entirely similar to that of compound **2** used as a pretreatment. Pretreatment of the cell surface with compounds **9** and **12** (MFI = 29.09 and 30.01, respectively) produced a slightly lower enhancement of binding affinity for 4C11, compared to those of compounds **2** and **7** as pretreatments. However, in the ITC experiments reported elsewhere,[10c] compound **9** (R = CF_3) has a high affinity for gp120, comparable to that of compound **2**, but compound **12** (R = NO_2) does not have significant affinity for gp120, indicating that these are not consistent with the current FACS studies, possibly due to the difference in the assay systems. Although the anti-HIV activity of **7** is weaker than that of compound **2**, the level of compound **7** inducing an enhancement of binding affinity of gp120 for 4C11 is comparable to that of compound **2**. The concentration of compounds used in the FACS analysis was 100 μM, much beyond the IC_{50} values of compounds **2** and **7**. A concentration of 100 μM would be also sufficient for the expression of anti-HIV activity caused by compounds **2** and **7**.

An effect on the use of compound **2** combined with another entry inhibitor was investigated. Analysis of the synergistic effects of anti-HIV agents was performed according to the median effect principle using the CalcuSyn version 2 computer program[18] to estimate IC_{50} values of compounds in different combinations. Combination indices (CI) were estimated from the data evaluated using the MTT assay

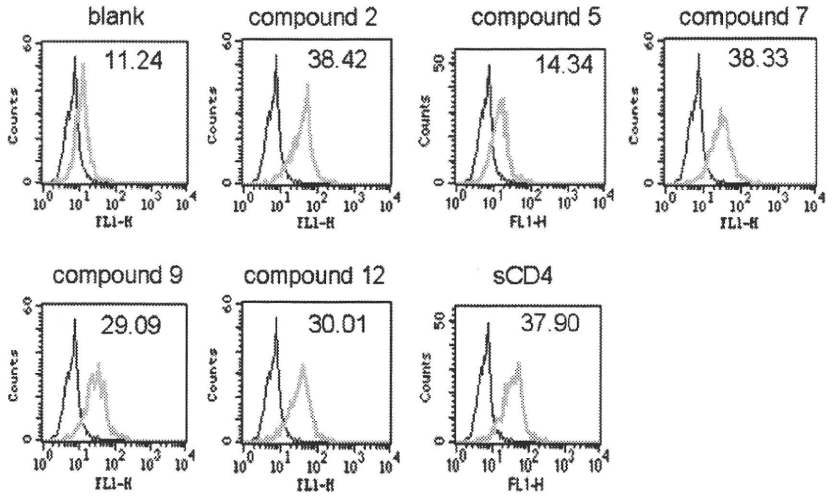

Figure 2. JR-FL (R5, Sub B) chronically infected PM1 cells were preincubated with 100 μM of a CD4 mimic or sCD4 (11 nM) for 15 min, and then incubated with an anti-HIV-1 mAb, 4C11, at 4 °C for 15 min. The cells were washed with PBS, and fluorescein isothiocyanate (FITC)-conjugated goat anti-human IgG antibody was used for antibody-staining. Flow cytometry data for the binding of 4C11 (green lines) to the Env-expressing cell surface in the presence of sCD4 or a CD4 mimic are shown among gated PM1 cells along with a control antibody (anti-human CD19: black lines). Data are representative of the results from a minimum of two independent experiments. The number at the top of each graph shows the mean fluorescence intensity (MFI) of the antibody 4C11.

Table 2
Combination indices (CI) for compound **2** or sCD4 and a CXCR4 antagonist, T140, against an HIV IIIB strain

Combination	HIV strain	CI values at different IC[a]		
		IC_{50}	IC_{75}	IC_{90}
2 + T140	IIIB	0.786	0.713	0.655
sCD4 + T140	IIIB	0.705	0.528	0.400

[a] The multiple-drug effect analysis reported by Chou et al. was used to analyze the effects of combinational uses of compounds.[18] CI <0.9: synergy, 0.9 < CI < 1.1: additivity, CI >1.1: antagonism.

(Table 2).[15] Compound **2** showed a highly remarkable synergistic anti-HIV activity with a co-receptor CXCR4 antagonist, T140,[8a] against an X4-HIV-1 strain, IIIB at various IC values (IC_{50}, IC_{75} and IC_{90}). However, sCD4 exhibited a higher synergistic effect (lower CI values) with T140 (Table 2). The interaction of sCD4 or a CD4 mimic with gp120 would expose the co-receptor-binding site of gp120, and the co-receptor CXCR4 could then easily approach gp120. Thus, an inhibitory effect of a CXCR4 antagonist would be meaningful, and a significant synergistic effect might also be brought about by a combination of sCD4 or a CD4 mimic and T140.

In summary, a series of CD4 mimic compounds were synthesized and evaluated for their anti-HIV activity. Several compounds showed significant anti-HIV activity with relatively low cytotoxicity. SAR studies showed that a certain level of size and electron-withdrawing ability of the substituents at the *p*-position of the phenyl ring are suitable for potent anti-HIV activity. In addition, the treatment of Env-expressing cells with several CD4 mimicking compounds causes a conformational change, exposing the co-receptor-binding site of gp120 externally. Thus, a CD4 mimic exhibited a remarkable synergistic effect with a co-receptor antagonist. These compounds are essential probes directed to the dynamic supramolecular mechanism of HIV entry, and important leads for the cocktail therapy of AIDS.

Acknowledgments

This work was supported by Mitsui Life Social Welfare Foundation, Grant-in-Aid for Scientific Research from the Ministry of Education, Culture, Sports, Science, and Technology of Japan, and Health and Labour Sciences Research Grants from Japanese Ministry of Health, Labor, and Welfare.

References and notes

1. Mitsuya, H.; Erickson, J. In *Textbook of AIDS Medicine*; Merigan, T. C., Bartlett, J. G., Bolognesi, D., Eds.; Williams & Wilkins: Baltimore, 1999; pp 751–780.
2. Chan, D. C.; Kim, P. S. *Cell* **1998**, *93*, 681.
3. (a) Alkhatib, G.; Combadiere, C.; Broder, C. C.; Feng, Y.; Kennedy, P. E.; Murphy, P. M.; Berger, E. A. *Science* **1996**, *272*, 1955; (b) Choe, H.; Farzan, M.; Sun, Y.; Sullivan, N.; Rollins, B.; Ponath, P. D.; Wu, L.; Mackay, C. R.; LaRosa, G.; Newman, W.; Gerard, N.; Gerard, C.; Sodroski, J. *Cell* **1996**, *85*, 1135; (c) Deng, H. K.; Liu, R.; Ellmeier, W.; Choe, S.; Unutmaz, D.; Burkhart, M.; Marzio, P. D.; Marmon, S.; Sutton, R. E.; Hill, C. M.; Davis, C. B.; Peiper, S. C.; Schall, T. J.; Littman, D. R.; Landau, N. R. *Nature* **1996**, *381*, 661; (d) Doranz, B. J.; Rucker, J.; Yi, Y. J.; Smyth, R. J.; Samson, M.; Peiper, S. C.; Parmentier, M.; Collman, R. G.; Doms, R. W. *Cell* **1996**, *85*, 1149; (e) Dragic, T.; Litwin, V.; Allaway, G. P.; Martin, S. R.; Huang, Y.; Nagashima, K. A.; Cayanan, C.; Maddon, P. J.; Koup, R. A.; Moore, J. P.; Paxton, W. A. *Nature* **1996**, *381*, 667.
4. Feng, Y.; Broder, C. C.; Kennedy, P. E.; Berger, E. A. *Science* **1996**, *272*, 872.
5. Wild, C. T.; Greenwell, T. K.; Matthews, T. J. *AIDS Res. Hum. Retroviruses* **1993**, *9*, 1051.
6. (a) Dorr, P.; Westby, M.; Dobbs, S.; Griffin, P.; Irvine, B.; Macartney, M.; Mori, J.; Rickett, G.; Smith-Burchnell, C.; Napier, C.; Webster, R.; Armour, D.; Price, D.; Stammen, B.; Wood, A.; Perros, M. *Antimicrob. Agents Chemother.* **2005**, *49*, 4721; (b) Price, D. A.; Armour, D.; De Groot, M.; Leishman, D.; Napier, C.; Perros, M.; Stammen, B. L.; Wood, A. *Bioorg. Med. Chem. Lett.* **2006**, *16*, 4633.
7. (a) Cahn, P.; Sued, O. *Lancet* **2007**, *369*, 1235; (b) Grinsztejn, B.; Nguyen, B.-Y.; Katlama, C.; Gatell, J. M.; Lazzarin, A.; Vittecoq, D.; Gonzalez, C. J.; Chen, J.; Harvey, C. M.; Isaacs, R. D. *Lancet* **2007**, *369*, 1261.
8. (a) Tamamura, H.; Xu, Y.; Hattori, T.; Zhang, X.; Arakaki, R.; Kanbara, K.; Omagari, A.; Otaka, A.; Ibuka, T.; Yamamoto, N.; Nakashima, H.; Fujii, N. *Biochem. Biophys. Res. Commun.* **1998**, *253*, 877; (b) Fujii, N.; Oishi, S.; Hiramatsu, K.; Araki, T.; Ueda, S.; Tamamura, H.; Otaka, A.; Kusano, S.; Terakubo, S.; Nakashima, H.; Broach, J. A.; Trent, J. O.; Wang, Z.; Peiper, S. C. *Angew. Chem., Int. Ed.* **2003**, *42*, 3251; (c) Tanaka, T.; Nomura, W.; Narumi, T.; Esaka, A.; Oishi, S.; Ohashi, N.; Itotani, K.; Evans, B. J.; Wang, Z.; Peiper, S. C.; Fujii, N.; Tamamura, H. *Org. Biomol. Chem.* **2009**, *7*, 3805.
9. Otaka, A.; Nakamura, M.; Nameki, D.; Kodama, E.; Uchiyama, S.; Nakamura, S.; Nakano, H.; Tamamura, H.; Kobayashi, Y.; Matsuoka, M.; Fujii, N. *Angew. Chem., Int. Ed.* **2002**, *41*, 2937.
10. (a) Zhao, Q.; Ma, L.; Jiang, S.; Lu, H.; Liu, S.; He, Y.; Strick, N.; Neamati, N.; Debnath, A. K. *Virology* **2005**, *339*, 213; (b) Schön, A.; Madani, N.; Klein, J. C.; Hubicki, A.; Ng, D.; Yang, X.; Smith, A. B., III; Sodroski, J.; Freire, E. *Biochemistry* **2006**, *45*, 10973; (c) Madani, N.; Schön, A.; Princiotto, A. M.; LaLonde, J. M.; Courter, J. R.; Soeta, T.; Ng, D.; Wang, L.; Brower, E. T.; Xiang, S.-H.; Do Kwon, Y.; Huang, C.-C.; Wyatt, R.; Kwong, P. D.; Freire, E.; Smith, A. B., III; Sodroski, J. *Structure* **2008**, *16*, 1689; (d) Haim, H.; Si, Z.; Madani, N.; Wang, L.; Courter, J. R.; Princiotto, A.; Kassa, A.; DeGrace, M.; McGee-Estrada, K.; Mefford, M.; Gabuzda, D.; Smith, A. B., III; Sodroski, J. *ProS Pathogens* **2009**, *5*, 1.
11. The structure of compound **2** was built in Sybyl and minimized with the MMFF94 force field and partial charges. (see: Halgren, T. A. *J. Comput. Chem.* **1996**, *17*, 490.) Docking was then performed using FlexSIS through its SYBYL

module, into the crystal structure of gp120 (PDB, entry 1RZJ). The binding site was defined as residues Val^{255}, Asp^{368}, Glu^{370}, Ser^{375}, Ile^{424}, Trp^{427}, Val^{430} and Val^{475}, and included residues located within a radius 4.4 Å. The ligand was considered to be flexible, and all other options were set to their default values. Figures were generated with ViewerLite version 5.0 (Accelrys Inc., San Diego, CA).

12. *For example, the synthesis of compound* **7**: To a solution of ethyl oxalyl chloride (0.400 mL, 3.48 mmol) in THF (20 mL) were added triethylamine (Et_3N) (0.480 mL, 3.48 mmol) and *p*-toluidine (373 mg, 3.48 mmol) with stirring at 0 °C. The reaction mixture was allowed to warm to room temperature, and then stirred for 6 h. After removal by filtration of the resulting salts, the filtrate was concentrated under reduced pressure. The residue was extracted with EtOAc (50 mL), and the extract was washed successively with brine (20 mL), 1 M HCl (20 mL × 2), brine (20 mL), saturated $NaHCO_3$ (20 mL × 2) and brine (20 mL × 3), then dried over $MgSO_4$. Concentration under reduced pressure gave the crude ethyl oxalamate, which was used without further purification. To a solution of the crude ethyl oxalamate (640 mg, 3.09 mmol) in THF (30 mL) were added aqueous 1 M NaOH (3.40 mL, 3.40 mmol), water (50 mL) and MeOH (20 mL) with stirring at 0 °C. The reaction mixture was allowed to warm to room temperature, and then stirred for 20 h. After the addition of aqueous 1 M HCl (5 mL), MeOH and THF were evaporated under reduced pressure. The residue was acidified to pH 2 with 1 M HCl, and extracted with EtOAc (50 mL × 2). The combined organic layer was washed with brine (20 mL × 3), and dried over $MgSO_4$. Concentration under reduced pressure gave the crude acid, which was used for the next reaction without further purification. To a solution of the above crude acid (514 mg, 2.87 mmol) in THF (10 mL) were added 1-hydoxybenzotriazole (484 mg, 3.16 mmol), 4-amino-2,2,6,6-tetramethylpiperidine (446 μL, 2.58 mmol), 1-ethyl-3-(3-dimethylaminopropyl)carbodiimide hydrochloride (606 mg, 3.16 mmol) and Et_3N (0.439 mL, 3.16 mmol) with stirring at 0 °C. The reaction mixture was allowed to warm to room temperature, and then stirred for 20 h. After evaporation of THF, the residue was dissolved in $CHCl_3$ (50 mL). The mixture was washed with saturated $NaHCO_3$ (20 mL × 2) and brine (20 mL × 3), and dried over $MgSO_4$. Concentration under reduced pressure gave the crude crystalline mass. The usual work-up followed by recrystallization from EtOAc–*n*-hexane gave the title compound **7** (363 mg, 1.14 mmol, 39.8%) as colorless crystals, mp = 176 °C; δ_H (400 MHz; $CDCl_3$) 1.07 (1H, m, NH), 1.16 (6H, s, CH_3), 1.29 (6H, s, CH_3), 1.44 (2H, m, CH_2), 1.91 (1H, d, *J* 3.7, C*H*H), 1.94 (1H, d, *J* 3.7, CH*H*), 2.34 (3H, s, CH_3), 4.25 (1H, m, CH), 7.17 (2H, d, *J* 8.3, ArH), 7.33 (1H, m, NH), 7.50 (2H, d, *J* 8.4, ArH), 9.18 (1H, s, NH); HRMS (FAB), *m*/*z* calcd for $C_{18}H_{28}N_3O_2$ $(MH)^+$ 318.2182, found 318.2173.
13. McFarland, C.; Vicic, D. A.; Debnath, A. K. *Synthesis* **2006**, 807.
14. *The synthesis of compound* **12**: To a solution of Et_3N (417 μL, 3.00 mmol) and 4-nitroaniline (138 mg, 1.00 mmol) in THF (1.3 mL) was added oxalyl dichloride (85.8 μL, 1.00 mmol) with stirring at 0 °C. After being stirred for 30 min at 0 °C, Et_3N (167 μL, 1.20 mmol) and 4-amino-2,2,6,6-tetramethylpiperidine (156 μL, 0.90 mmol) were added. The reaction mixture was stirred for 6 h at 0 °C. After removal by filtration of the resulting salts, the filtrate was concentrated under reduced pressure. The residue was dissolved in $CHCl_3$ (20 mL), and the mixture was washed successively with brine (10 mL), saturated $NaHCO_3$ (10 mL × 2) and brine (10 mL × 3), and dried over $MgSO_4$. Concentration under reduced pressure followed by flash chromatography over silica gel with $CHCl_3$–MeOH (9:1) gave 42.4 mg (0.122 mmol, 13.5%) of the title compound **12** as colorless crystals, mp = 190 °C; δ_H (400 MHz; $CDCl_3$) 1.09 (1H, m, NH), 1.17 (6H, s, CH_3), 1.29 (6H, s, CH_3), 1.43 (2H, m, CH_2), 1.92 (1H, d, *J* 3.8, C*H*H), 1.95 (1H, d, *J* 3.8, CH*H*), 4.28 (1H, m, CH), 7.29 (1H, m, NH), 7.82 (2H, d, *J* 9.1, ArH), 8.28 (2H, d, *J* 9.1, ArH), 9.55 (1H, s, NH); HRMS (FAB), *m*/*z* calcd for $C_{17}H_{25}N_4O_4$ $(MH)^+$ 349.1876, found 349.1871.
15. Yoshimura, K.; Shibata, J.; Kimura, T.; Honda, A.; Maeda, Y.; Koito, A.; Murakami, T.; Mitsuya, H.; Matsushita, S. *AIDS* **2006**, *20*, 2065.
16. (a) Chapman, N. B.; Shorter, J. *Advances in Linear Free Energy Relationship*; Plenum Press: London, 1972; (b) Chapman, N. B.; Shorter, J. *Correlation Analysis in Chemistry*; Plenum Press: London, 1978; (c) Hansch, C.; Leo, A. J.; Hoekman, D. *Exploring QSAR, Hydrophobic, Electronic, and Steric Constants*; American Chemical Society: Washington, DC, 1995.
17. Taft, R. W. In *Steric Effects in Organic Chemistry*; Newman, M. S., Ed.; John Wiley: New York, 1956; p 556.
18. (a) Chou, T. C.; Talalay, P. *J. Biol. Chem.* **1977**, *252*, 6438; (b) Chou, T. C.; Hayball, M. P. *CalcuSyn*, 2nd ed.; Biosoft: Cambridge, UK, 1996.

Remodeling of Dynamic Structures of HIV-1 Envelope Proteins Leads to Synthetic Antigen Molecules Inducing Neutralizing Antibodies

Toru Nakahara,[†] Wataru Nomura,*[,†] Kenji Ohba,[‡] Aki Ohya,[†] Tomohiro Tanaka,[†] Chie Hashimoto,[†] Tetsuo Narumi,[†] Tsutomu Murakami,[‡] Naoki Yamamoto,[‡] and Hirokazu Tamamura*[,†]

Department of Medicinal Chemistry, Institute of Biomaterials and Bioengineering, Tokyo Medical and Dental University, 2-3-10 Kandasurugadai, Chiyoda-ku, Tokyo 101-0062, Japan, and AIDS Research Center, National Institute of Infectious Diseases, 1-23-1 Toyama, Shinjuku-ku, Tokyo 162-8640, Japan. Received November 16, 2009; Revised Manuscript Received February 28, 2010

A synthetic antigen targeting membrane-fusion mechanism of HIV-1 has a newly designed template with C3-symmetric linkers mimicking N36 trimeric form. The antiserum produced by immunization of the N36 trimeric form antigen showed structural preference in binding to N36 trimer and stronger inhibitory activity against HIV-1 infection than the N36 monomer. Our results suggest an effective strategy of HIV vaccine design based on a relationship to the native structure of proteins involved in HIV fusion mechanisms.

INTRODUCTION

Antibody-based therapy is one of the promising treatments for AIDS. In recent years, AIDS antibodies have been produced by immunization (*1*) and by de novo engineering of monoclonal antibodies (mAb) with molecular evolution tactics such as phage display (*2*). Despite enormous efforts, however, only a limited number of highly and broadly HIV-neutralizing human mAbs have been isolated and characterized. These antibodies include gp41 Abs, 2F5 (*3*–*6*) and 4E10 (*5*–*7*), and gp120 Abs, 2G12 (*8*) and b12 (*9*). gp41 is a transmembrane envelope glycoprotein, which is divided into an endodomain and an ectodomain by the transmembrane region; the latter contains a hydrophobic amino-terminal fusion peptide, followed by amino-terminal and carboxy-terminal leucine/isoleucine heptad repeat domains with helical structures (HR1 and HR2, respectively). In the membrane fusion process of HIV-1, these subunits form a "pre-bundle" complex. The HR1 and HR2 regions are termed the N-terminal helix (N36) and C-terminal helix (C34), respectively. These helices form a six-helical bundle consisting of a central parallel trimeric coiled-coil of N36 surrounded by C34 in an antiparallel hairpin fashion. In design of immunogens that elicit broadly neutralizing antibodies, a useful strategy is to produce molecules that mimic the natural trimer on the virion surface. Previous studies show that these molecules could be proteins expressed as a recombinant form or on the surface of particles such as pseudovirions or proteoliposomes (*10*–*12*). The X-ray crystallographic study of gp41 shows that the distances between any two residues at the N-terminus of N-region are almost equal at approximately 10 Å (Figure 1A). A chemically synthetic template could be useful in connection with the design of a peptidomimetic corresponding to the native structure of gp41. To date, several gp41 mimetics have been synthesized as inhibitors or antigens and subjected to inhibition or neutralization assays (*13*–*16*). However, the templates for assembly of these helical peptides contain branched peptide linkers, which are not exactly equivalent in length (*14*). The N-terminal peptides constrained by another threefold linker showed high affinity for C-terminal peptides, although its biological advantages have not been determined (*15*). The mimicry can be estimated using the broadly neutralizing mAbs; suitable mimetics will bind neutralizing mAbs efficiently, but they will bind non-neutralizing mAbs poorly. In the present study, we designed and synthesized a novel three-helical bundle mimetic, which corresponds to the trimeric form of N36. We investigated whether mice immunized with the equivalent trimeric form of N36 mimetic can produce antibodies with stronger binding affinity for N36 trimer than for N36 monomer. This approach demonstrates the possibility of producing structure-specific antibodies by immunization of synthetic antigens corresponding to the natural form of viral proteins.

EXPERIMENTAL PROCEDURES

Conjugation of N36REGC and the Template to Produce triN36e. Compound **6** (100 μg, 0.174 μmol) and N36REGC (3.4 mg, 0.574 μmol) were dissolved in a mixture of 300 μL of 200 mM acetate buffer (pH 5.2) and 300 μL of TFE under a nitrogen atmosphere, then TCEP·HCl was added. The reaction was stirred for 72 h at room temperature and monitored by HPLC. The ligation product (triN36e) was separated as an HPLC peak and was characterized by ESI-TOF-MS, *m/z* calcd for $C_{690}H_{1160}N_{226}O_{201}S_3$ 15933.1, found 15933.8. The purification was performed by reverse phase HPLC (YMC-Pack ODS-A column, 10 × 250 mm). Elution was carried out with a 40–50% linear gradient of acetonitrile (0.1% TFA) over 50 min. Purified triN36e, obtained in 16% yield, was identified by ESI-TOF-MS. The detailed synthesis of peptides is described in the Supporting Information (SI).

CD Spectra. CD measurements were performed with a J-720 circular dichroism spectrolarimeter equipped with a thermoregulator (JASCO). The wavelength dependence of molar ellipticity [θ] was monitored at 25 °C from 190 to 250 nm. Peptides were dissolved in 20 mM acetate buffer (pH 4.0) containing 40% MeOH (*23*, *24*). The experimental helicity was calculated as reported previously (*17*–*19*).

Immunization and Sample Collection. Six-week-old male BALB/c mice were purchased from Sankyo Laboratory Service Corp. (Tokyo, Japan) and maintained under specific pathogen-free conditions in an animal facility. The experimental protocol was approved by the ethical review committee of Tokyo Medical and Dental University. Freund incomplete adjuvant and PBS

* To whom correspondence should be addressed. E-mail: nomura.mr@tmd.ac.jp; tamamura.mr@tmd.ac.jp. phone: +81-3-5280-8036, fax: +81-3-5280-8039.
[†] Tokyo Medical and Dental University.
[‡] National Institute of Infectious Diseases.

10.1021/bc900502z
Published on Web 04/01/2010

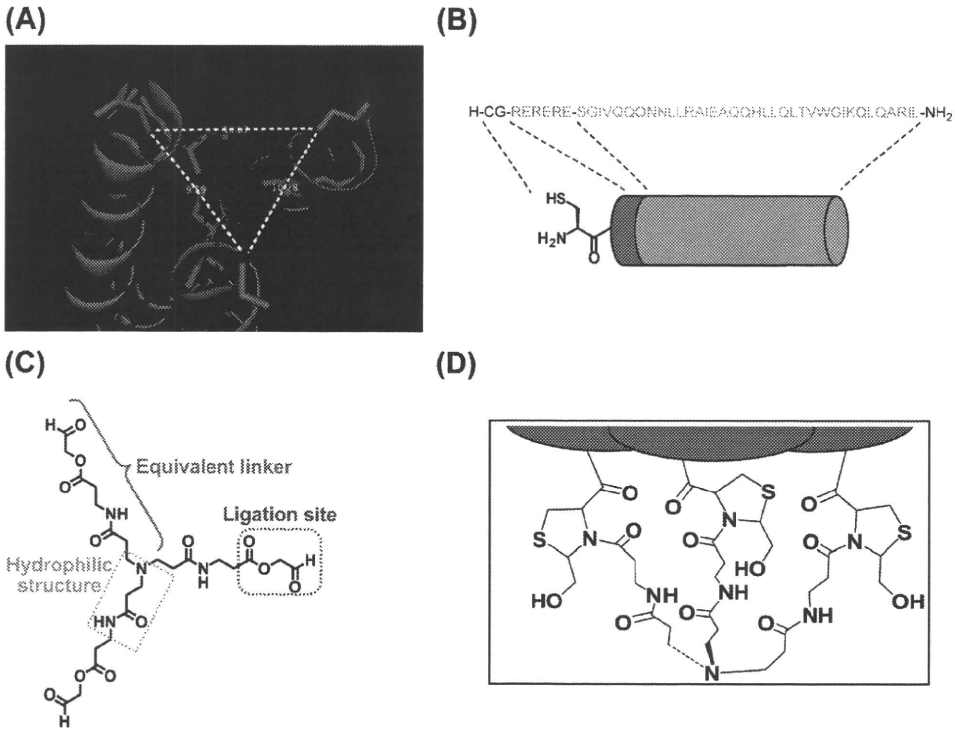

Figure 1. (A) Distances between hydrogen atoms for hydroxyl groups in N-terminal serine residues of N36 helices in trimeric form. The distances were evaluated by PyMOL (*21*). (B) Cartoon presentation of each N36 derived peptide, N36REGC. (C) Design of a C3-symmetric template. The amino acid residues are described in single letters. (D) Conjugated structure of trimeric N36 after thiazolidine ligation.

were purchased from Wako Pure Chemical Industries (Osaka, Japan). DMSO (endotoxin free) was purchased from Sigma-Aldrich (St. Louis, MO).

All mice were bled one week before immunization. One hundred micrograms of antigen was dissolved in 1 μL of DMSO. The solution was mixed with 50 μL of PBS and 50 μL of Freund incomplete adjuvant. The mixture was injected subcutaneously under anesthesia on days 0, 14, 28, 42, and 58. Mice were bled on days 21, 35, 49, and 65. Serum was separated by centrifugation (15 000 rpm) at 4 °C for 15 min and inactivated at 56 °C for 30 min. Sera were stored at −80 °C before use.

Serum Titer ELISA. Tween-20 (polyoxyethylene (20) sorbitan monolaurate) and hydrogen peroxide (30%) were purchased from Wako. ABTS (2,2-azino-bis(3-ethylbenzothiazoline-6-sulfonic acid) diammonium salt) was purchased from Sigma-Aldrich. Antimouse IgG (H+L)(goat)-HRP was purchased from EMD Chemicals (San Diego, CA). Ninty-six-well microplates were coated with 25 μL of a synthetic peptide at 10 μg/mL in PBS at 4 °C for overnight. The coated plates were washed 10 times with deionized water and blocked with 150 μL of blocking buffer (0.02% PBST, PBS with 0.02% Tween 20, containing 5% skim milk) at 37 °C for 1 h. The plates were washed with deionized water 10 times. Mice sera were diluted in 0.02% PBST with 1% skim milk, and 50 μL of 2-fold serial dilutions of sera from 1/200 to 1/102400 were added to the wells and allowed to incubate at 37 °C for 2 h. The plates were washed 10 times with deionized water. Twenty-five microliters of HRP-conjugated antimouse IgG, diluted 1:2000 in 0.02% PBST, was added to each well. After 45 min incubation, the plates were washed 10 times and 25 μL of HRP substrate, prepared by dissolving 10 mg ABTS to 200 μLof HRP staining buffer—a mixture of 0.5 M citrate buffer (pH 4.0, 1 mL), H_2O_2 (3 μL), and H_2O (8.8 mL)—was added. After 30 min incubation, the reaction was stopped by addition of 25 μL/well 0.5 M H_2SO_4, and optical densities were measured at 405 nm.

Virus Preparation. The pNL4-3 construct (8 μg) was transfected into 293T cells by Lipofectamine LTX (Invitrogen, Carlsbad, CA) followed by changing medium at 12 h after transfection. At 48 h after changing medium, the supernatant was collected, passed through a 0.45 μm filter, and stored at −80 °C as HIV-1_{NL4-3} strain before use. For titration, MT-4 cells were infected with serially 3-fold diluted virus from 1/10 to 1/196830, and cultured for 7 days. HIV-1 p24 levels in supernatants were measured, and then the titer of virus solution was calculated.

Anti-HIV Assay. Virus was prepared as described above except that the transfection of pNL4-3 was performed by the calcium phosphate method. Anti-HIV-1 activity was determined on the basis of protection against HIV-1-induced cytopathogenicity in MT-4 cells. Various concentrations of AZT, N36RE, and triN36e (The starting concentrations are 100, 10, and 1 μM, respectively) were added to HIV-1-infected MT-4 cells (MOI = 0.01) by 2-fold serial dilution and placed in wells of a flat-bottomed microtiter plate (2.0×10^4 cells/well). After 5 days' incubation at 37 °C in a CO_2 incubator, the number of viable cells was determined using the 3-(4,5-dimethylthiazol-2-yl)-2,5-diphenyltetrazolium bromide (MTT) method (EC_{50}). Cytotoxicity of compounds was determined on the basis of viability of mock-infected cells using the MTT method (CC_{50}). Each experiment was performed three times independently.

Neutralizing Assay. MT4-cells (1×10^5 cells/100 μL) were incubated in 100 μL medium containing 10 μL sera from immunized or preimmunized mice for 1 h at 37 °C, then pretreated MT-4 cells were infected with HIV-1_{NL4-3} (MOI = 0.05). At 3 days after infection, cells were collected by centrifuge at 4000 rpm for 10 min at 4 °C. After discarding supernatant, pellets were lysed with 30 μL of lysis buffer (50 mM Tris·HCl (pH 7.5), 150 mM NaCl, 1% NP-40), then 30 μL of 2 × SDS buffer (125 mM Tris·HCl (pH 6.8), 4% SDS, 20% glycerol, 10% 2-ME, 0.004% BPB) were added and boiled for 10 min. The samples (5 μL) were subjected to SDS-page to perform Western blotting. The HIV-1 gag p24 was detected by using Western lightning ECL kit (PerkinElmer, MA) according to manufacturer's instruction after treatment of HIV-1 p24

Scheme 1. Synthesis of the Equivalently Branched Template 6

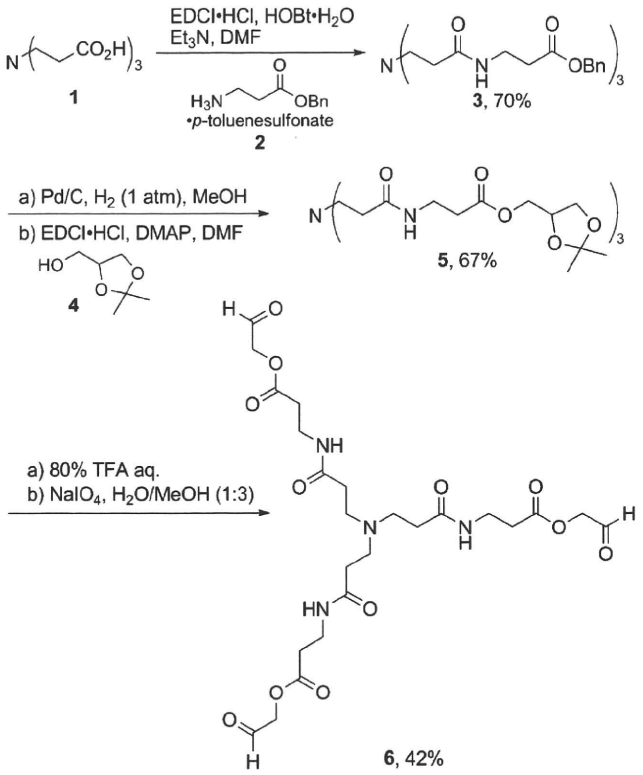

antibody (2C2; 1:2000 dilution) (*20*) and anti- mouse IgG (H+L)-HRP (Millipore, MA). The band intensity of p24 was calculated with post/pre-immunized samples by using *ImageJ* image analyzing software.

RESULTS AND DISCUSSION

The N-region of gp41 is known to be an aggregation site involving a trimeric coiled-coil conformation. In design of an N36-derived peptide (N36RE), the triplet repeat of arginine and glutamic acid was fused to the N-terminus to increase the solubility in buffer solution (Figure 1B). In order to form a triple helix corresponding precisely to the gp41 prefusion form, we designed the novel C3-symmetric template depicted in Figure 1C. This designed template linker has three branches of equal length and possesses the hydrophilic structure and ligation site for coupling with N36RE. The template was synthesized from the commercially available 3-[bis(2-carboxyethyl)amino]propanoic acid **1** as shown in Scheme 1. Coupling of **1** with β-alanine benzyl ester **2** gave the corresponding triamide **3** in 77% yield. Cleavage of three benzyl esters by hydrogenation and coupling with solketal **4** produced the corresponding triester **5**. Deprotection of the acetonides with aqueous 80% TFA followed by oxidative cleavage of diol group led to the desired template **6**. This approach uses thiazolidine ligation for chemoselective coupling of Cys-containing unprotected N36RE (N36REGC) with a three-armed aldehyde scaffold producing triN36e (Figure 1D). Thiazolidine ligation is a peptide segment coupling strategy which does not require side chain protecting groups (*22*−*26*). The reaction consists of three steps: (i) aldehyde introduction, in which a masked glycolaldehyde ester is linked to the carboxyl terminus of an unprotected peptide by reverse proteolysis; (ii) ring formation, in which the unmasked aldehyde reacts at acidic pH with the α-amino group of an N-terminal cysteine residue of the second unprotected peptide forming a thiazolidine ring; and (iii) rearrangement at higher pH in which O-acyl ester linkage is converted to an N-acyl amide linkage forming a peptide bond with a pseudoproline structure (Figure 2).

Circular dichroism (CD) spectra of triN36e and N36RE, which is a monomer form without N-terminal Cys-Gly residues, are shown in Figure 3A. The peptides were dissolved in 20 mM acetate buffer with 40% MeOH, pH4.0, suitable for measurement of CD spectra of membrane proteins (*27, 28*). Both spectra display double minima at 208 and 222 nm and showed high molar ellipticity as absolute values (Table 1). The results indicate that these peptides form a highly structured α-helix and that the helical content of the trimer triN36e is higher than that of the monomer N36RE. Furthermore, to assess the interaction of triN36e with C34, CD spectra of the peptide mixture with C34-derived peptide, C34RE, were measured (Figure 3B,C). The spectrum of triN36e and C34RE mixture showed high molecular ellipticity as an absolute value comparable with that of triN36e alone. This supports the conclusion that C34RE interacts with tri36e and thereby induces a higher helical form as shown previously (*29*).

Mice were immunized with these synthetic gp41 mimetics and antibody production was successfully induced (the detailed titer increase in 5 weeks' immunization is given in the Supporting Information). Two out of three mice showed induction of antibodies against either antigen (N36RE or triN36e). Antibody titers and selectivity of antisera isolated from mice immunized with N36RE or triN36e were evaluated by serum titer ELISA against coated synthetic antigens. The most active antiserum for each antigen was utilized for the evaluation of binding activity by ELISA (Figure 4). The N36RE-induced antibody showed approximately 5 times higher affinity for N36RE than for triN36e, as 50% bound serum dilutions are 3.88×10^{-4} and 2.14×10^{-3} to N36RE and triN36e, respectively. It is noteworthy that the triN36e-induced antibody showed approximately 30 times higher preference in binding affinity for triN36e antigen than for N36RE (serum dilutions at 50% bound are 3.83×10^{-3} to N36RE and 1.33×10^{-4} to triN36e). Although this evaluation was not determined with purified mAbs, it is clear that the antibodies produced exploit a structural preference for antigens. The mechanism of induction

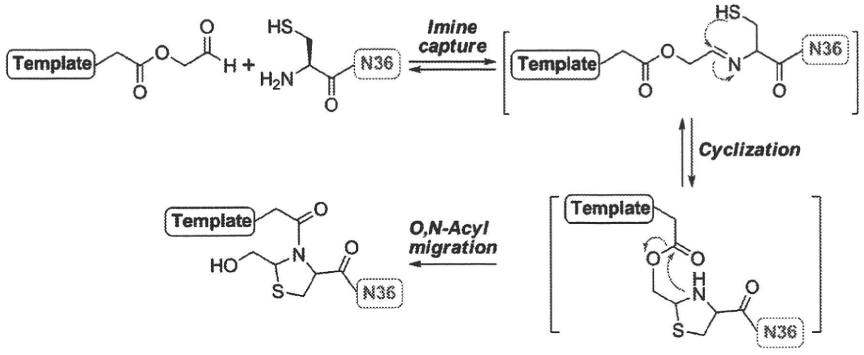

Figure 2. Reaction mechanisms of thiazolidine ligation utilized for assembly of N36RE helices on the template.

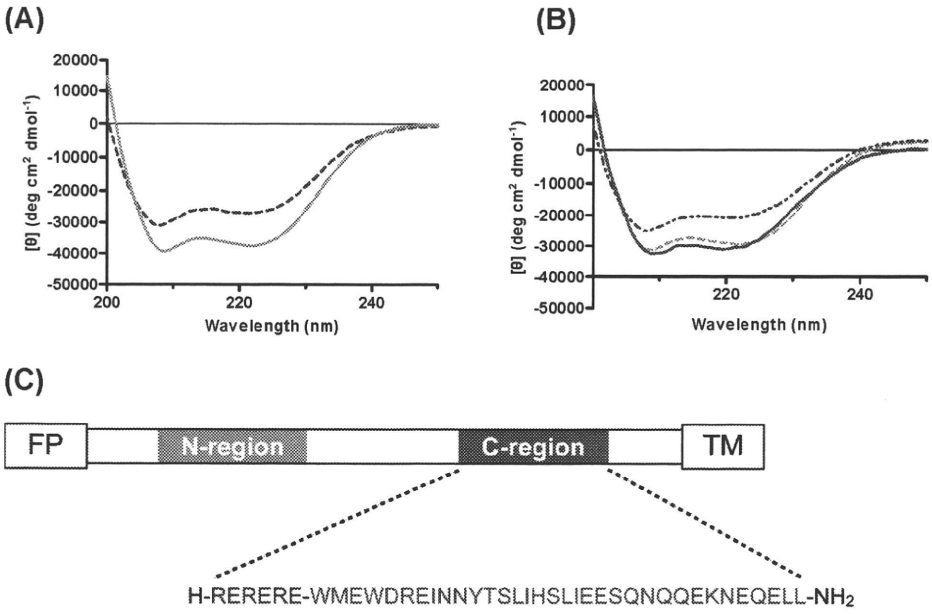

Figure 3. (A) Circular dichroism (CD) spectra of N36RE and triN36e. In the spectra, a blue dashed line and a green line show N36RE (monomer) and triN36e (trimer), respectively. Concentrations of the peptides are 10 and 3.3 μM for N36RE and triN36e, respectively. (B) CD spectra in the presence or absence of C34RE peptide. The spectra show the following: a dashed green line, triN36e; a dashed blue line, C34RE; a red line, triN36e+C34RE, respectively. The concentrations of peptides were as follows: triN36e (2.3 μM), C34-derived peptide C34RE (7 μM), and mixture of both peptides (3.5 μM each). (C) The amino acid sequence of C34RE described in single letters. FP and TM represent hydrophobic fusion peptide and transmembrane domain, respectively.

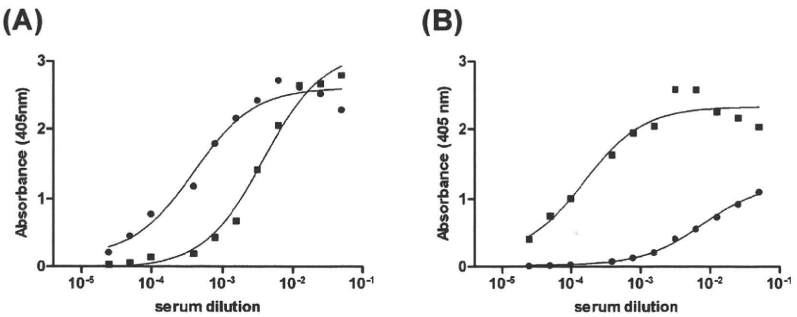

Figure 4. Serum titers of antibodies produced by N36 monomer and conformationally constrained N36 trimeric antigen. The titers were evaluated against N36RE (monomer) (A) and triN36e (trimer) (B). The plots indicate the results of sera obtained from N36RE-immunized mouse (•) and triN36e-immunized mouse (■).

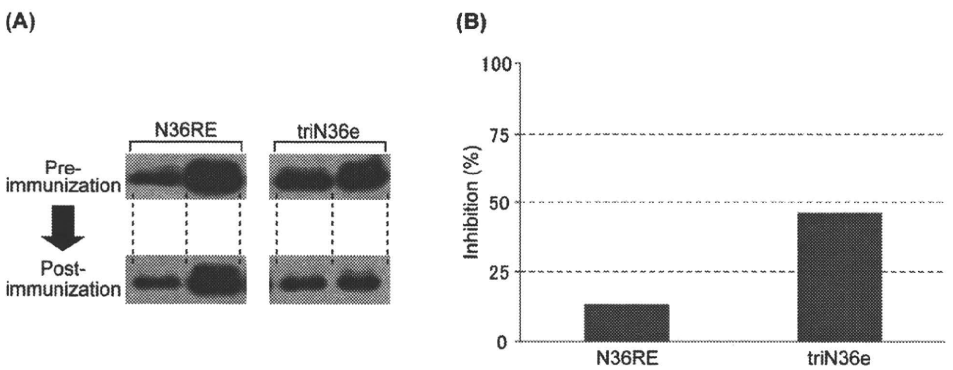

Figure 5. Determination of neutralization activity of the antibodies produced by immunization of peptidomimetic antigens. (A) Results of p24 assay to evaluate inhibition for HIV-1 infection by produced antibodies. Preimmunization sera were used as control. Experiments were duplicated. (B) Average % inhibition of p24 production calculated from the band intensities in panel (A).

of structure-specific antibody is still not clear, but the results could suggest the efficacy of producing antibodies with structural specificity and that the synthesis of structure-involving antigens is an effective strategy when higher specificity is required.

Neutralizing activity of sera against HIV-1 infection was assessed by p24 assays utilizing antisera from two mice that showed antibody production for each antigen (Figure 5). Sera

Table 1. Differences of α-Helicities between N36RE and triN36e Calculated from CD Spectra in Figure [3]

	$[\theta]_{222}$	$[\theta]_{222}/[\theta]_{208}$	α-helicity
N36RE	−30 957	0.87	73%
triN36e	−38 998	0.96	95%

Table 2. EC_{50} and CC_{50} Values Calculated from Inhibition Assays of Peptidomimetics

	AZT	triN36e	N36RE
EC_{50} (μM)[a]	0.047	0.49	1.4
CC_{50} (μM)[b]	>50	>1	>10

[a] EC_{50} values are based on the inhibition of HIV-induced cytopathogenicity in MT-4 cells. [b] CC_{50} values are based on the reduction of the viability of MT-4 cells. All data are the mean values for at least three experiments.

from mice immunized with the same antigen showed similar inhibitory activity against viral infection (12.5% and 14.8% for N36RE, 40.3% and 52.1% for triN36e). A trend was observed that the sera from triN36e immunization shows higher inhibition than those from N36RE immunization. This suggests that the synthetic antigen corresponding to the N36 trimeric form induces antibody with neutralization activity superior to that of the monomer peptide antigen and implies a restricted response of B-cells upon immunization to the trimeric form of N36RE. In order to assess the compatibility of induced antibodies in HIV-1 entry inhibition, the HIV-1 inhibitory activities of peptidomimetics (N36RE and triN36e) have been evaluated by viral infection and cytotoxicity assays. A C-terminal region peptide known as Enfuvirtide (T20, Roche/Trimeris) has been used clinically as a fusion inhibitor, and its success indicates that gp41-derived peptides might be potent inhibitors, useful against HIV-1 infection (*30*). In the development of anti-HIV peptides, several mimetics such as Enfuvirtide, CD4 binding site of gp120 (*31*), and protein-nucleic acid interactions (*32*), which disrupt protein−protein interactions, have been produced. As indicated in Table 2, N36 and triN36e showed modest inhibitory activity as reported in previous studies (*33*−*35*). The potency of triN36e was three times higher than that of N36RE indicating that the active structure of monomer N36RE is a trimeric form. Cytotoxicity of the antigens was not observed at concentrations of 1 μM of triN36e and 10 μM of N36RE.

CONCLUSIONS

In summary, a mimic of HIV-1 gp41-N36 designed as a new vaccine has been synthesized utilizing a novel template with three branched linkers of equal lengths. Thiazolidine-forming ligation attached the esteraldehyde of three-branched template with N-terminal cysteine of peptides in an aqueous medium. The resulting peptide antigen successfully induces antibodies with neutralization activity against HIV-1 infection. It is of special interest that the antibody produced acquires structural preference to antigen, which showed 30 times higher binding affinity for trimer than for monomer. This indicates the effectiveness of the design based on the structural dynamics of HIV-1 fusion mechanism of an antigen which could elicit neutralizing antibodies. In a design based on the N36 region of gp41, the exposed timing of epitopes is limited during HIV-1 entry (*36*), and carbohydrates, which could make accession of antibodies to epitopes difficult, are not associated with the amino acid residues of the native protein. These two advantages could further enhance the potential of a vaccine design based on the N36 region. During preparation of the manuscript, a new HIV vaccine strategy was reported by Burton's group (*37*). The report describes the importance of antibody recognition for the trimer form of surface protein. The trimer-specific antibodies indicate broad and potent neutralization. The gp41 trimer-form specific antibody produced in this study could also obtain the corresponding properties. The elucidation of antibody-producing mechanisms and epitope recognition mode of antibodies in antiserum during HIV-1 entry will be addressed in future studies.

ACKNOWLEDGMENT

The authors deeply thank Prof. K. Akiyoshi (Tokyo Medical and Dental Univ.) for allowing access to CD spectroporalimeter.

Supporting Information Available: HPLC chromatograms and NMR charts of compounds **3**, **5**, and **6**. Results of ESI-TOF-MS, and HPLC chromatograms of peptides N36RE, N36REGC, and triN36e. Results of serum titer ELISA of antisera collected during immunization. This material is available free of charge via the Internet at http://pubs.acs.org.

LITERATURE CITED

(1) Cabezas, E., Wang, M., Parren, P. W. H. I., Stanfield, R. L., and Satterthwait, A. C. (2000) A structure-based approach to a synthetic vaccine for HIV-1. *Biochemistry 39*, 14377–14391.

(2) Burton, D. R., Barbas, C. F., III, Persson, M. A. A., Koenig, S., Chanock, R. M., and Lerner, R. A. (1991) A large array of human monoclonal antibodies to type 1 human immunodeficiency virus from combinatorial libraries of asymptomatic seropositive individuals. *Proc. Natl. Acad. Sci. U.S.A. 88*, 10134–10137.

(3) Conley, A. J., Kessler, J. A. II, Boots, L. J., Tung, J. S., Arnold, B. A., Keller, P. M., Shaw, A. R., and Emini, R. A. (1994) Neutralization of divergent human immunodeficiency virus type 1 variants and primary isolates by IAM-41−2F5, an anti-gp41 human monoclonal antibody. *Proc. Natl. Acad. Sci. U.S.A. 91*, 3348–3352.

(4) Ofek, G., Tang, M., Sambor, A., Katinger, H., Mascola, J. R., Wyatt, R., and Kwong, P. D. (2004) Structure and mechanistic analysis of the anti-human immunodeficiency virus type 1 antibody 2F5 in complex with its gp41 epitope. *J. Virol. 78*, 10724–10737.

(5) Alam, S. M., McAdams, M., Boren, D., Rak, M., Scearce, R. M., Gao, F., Camacho, Z. T., Gewirth, D., Kelsoe, G., Chen, P., and Haynes, B. F. (2007) The role of antibody polyspecificity and lipid reactivity in binding of broadly neutralizing anti-HIV-1 envelope human monoclonal antibodies 2F5 and 4E10 to glycoprotein 41 membrane proximal envelope epitopes. *J. Immunol. 178*, 4424–4435.

(6) Nelson, J. D., Brunel, F. M., Jensen, R., Crooks, E. T., Cardoso, R. M. F., Wang, M., Hessell, A., Wilson, I. A., Binley, J. M., Dawson, P. E., Burton, D. R., and Zwick, M. B. (2007) An affinity-enhanced neutralizing antibody against the membrane-proximal external region of human immunodeficiency virus type 1 gp41 recognizes an epitope between those of 2F5 and 4E10. *J. Virol. 81*, 4033–4043.

(7) Cardoso, R. M. F., Zwick, M. B., Stanfield, R. L., Kunert, R., Binley, J. M., Katinger, H., Burton, D. R., and Wilson, I. A. (2005) Broadly neutralizing anti-HIV antibody 4E10 recognizes a helical conformation of a highly conserved fusion-associated motif in gp41. *Immunity 22*, 163–173.

(8) Trkola, A., Purtscher, M., Muster, T., Ballaun, C., Buchacher, A., Sullivan, N., Srinivasan, K., Sodroski, J., Moore, J. P., and Katinger, H. (1996) Human monoclonal antibody 2G12 defines a distinctive neutralization epitope on the gp120 glycoprotein of human immunodeficiency virus type 1. *J. Virol. 70*, 1100–1108.

(9) Pantophlet, R., Saphire, E. O., Poignard, P., Parren, P. W. H. I., Wilson, I. A., and Burton, D. R. (2003) Fine mapping of the interaction of neutralizing and nonneutralizing monoclonal antibodies with the CD4 binding site of human immunodeficiency virus type 1 gp120. *J. Virol. 77*, 642–658.

(10) Sanders, R. W., Vesanen, M., Schuelke, N., Master, A., Schiffner, L., Kalyanaraman, R., Paluch, M., Berkhout, B., Maddon, P. J., Olson, W. C., Lu, M., and Moore, J. P. (2002) Stabilization of the soluble, cleaved, trimeric form of the envelope glycoprotein complex of human immunodeficiency virus type 1. *J. Virol. 76*, 8875–8889.

(11) Yang, X., Wyatt, R., and Sodroski, J. (2001) Improved elicitation of neutralizing antibodies against primary human immunodeficiency viruses by soluble stabilized envelope glycoprotein trimers. *J. Virol. 75*, 1165–1171.

(12) Grundner, C., Mirzabekov, T., Sodroski, J., and Wyatt, R. (2002) Solid-phase proteoliposomes containing human immunodeficiency virus envelope glycoproteins. *J. Virol. 76*, 3511–3521.

(13) De Rosny, E., Vassell, R., Wingfield, R. T., Wild, C. T., and Weiss, C. D. (2001) Peptides corresponding to the heptad repeat motifs in the transmembrane protein (gp41) of human immunodeficiency virus type 1 elicit antibodies to receptor-activated conformations of the envelope glycoprotein. *J. Virol. 75*, 8859–8863.

(14) Tam, J. P., and Yu, Q. (2002) A facile ligation approach to prepare three-helix bundles of HIV fusion-state protein mimetics. *Org. Lett. 4*, 4167–4170.

(15) Xu, W., and Taylor, J. W. (2007) A template-assembled model of the N-peptide helix bundle from HIV-1 gp-41 with high affinity for C-peptide. *Chem. Biol. Drug Des. 70*, 319–328.

(16) Louis, J. M., Nesheiwat, I., Chang, L., Clore, G. M., and Bewlet, C. A. (2003) Covalent trimers of the internal N-terminal trimeric coiled-coil of gp41 and antibodies directed against them are potent inhibitors of HIV envelope-mediated cell fusion. *J. Biol. Chem. 278*, 20278–20285.

(17) Chen, Y.-H., Yang, J. T., and Chau, K. H. (1974) Determination of the helix and β form of proteins in aqueous solution by circular dichroism. *Biochemistry 13*, 3350–3359.

(18) Gans, P. J., Lyu, P. C., Manning, M. C., Woody, R. W., and Kallenbach, N. R. (1991) The helix-coil transition in heterogeneous peptides with specific side-chain interactions: theory and comparison with CD spectral data. *Biopolymers 13*, 1605–1614.

(19) Jackson, D. Y., King, D. S., Chmielewski, J., Singh, S., and Schultz, P. G. (1991) A general approach to the synthesis of short alpha-helical peptides. *J. Am. Chem. Soc. 113*, 9391–9392.

(20) Ohba, K., Ryo, A., Dewan, M. Z., Nishi, M., Naito, T., Qi, X., Inagaki, Y., Nagashima, Y., Tanaka, Y., Okamoto, T., Terashima, K., and Yamamoto, N. (2009) Follicular dendritic cells activate HIV-1 replication in monocytes/macrophages through a juxtacrine mechanism mediated by P-selectin glycoprotein ligand 1. *J. Immunol. 183*, 524–532.

(21) Liu, J., Shu, W., Fagan, M. B., Nunberg, J. H., and Lu, H. (2001) Structural and functional analysis of the HIV gp41 core containing an Ile573 to Thr substitution: implications for membrane fusion. *Biochemistry 40*, 2797–2807.

(22) Liu, C. F., and Tam, J. P. (1994) Peptide segment ligation strategy without use of protecting groups. *Proc. Natl. Acad. Sci. U.S.A. 91*, 6584–6588.

(23) Tam, J. P., and Miao, Z. (1999) Stereospecific pseudoproline ligation of N-terminal serine, threonine, or cysteine-containing unprotected peptides. *J. Am. Chem. Soc. 121*, 9013–9022.

(24) Tam, J. P., Yu, Q., and Yang, J.-L. (2001) Tandem ligation of unprotected peptides through thiaprolyl and cysteinyl bonds in water. *J. Am. Chem. Soc. 123*, 2487–94.

(25) Eom, K. D., Miao, Z., Yang, J.-L., and Tam, J. P. (2003) Tandem ligation of multipartite peptides with cell-permeable activity. *J. Am. Chem. Soc. 125*, 73–82.

(26) Sadler, K., Zhang, Y., Xu, J., Yu, Q., and Tam, J. P. (2008) Quaternary protein mimetics of gp41 elicit neutralizing antibodies against HIV fusion-active intermediate state. *Biopolym. (Pept. Sci.) 90*, 320–329.

(27) Bychkova, V. E., Dujsekina, A. E., Klenin, S. I., Tiktopulo, E. I., Uversky, V. N., and Ptitsyn, O. B. (1996) Molten globule-like state of cytochrome *c* under conditions simulating those near the membrane surface. *Biochemistry 35*, 6058–6063.

(28) Nishi, K., Komine, Y., Sakai, N., Maruyama, T., and Otagiri, M. (2005) Cooperative effect of hydrophobic and electrostatic forces on alcohol-induced α-helix formation of α_1-acid glycoprotein. *FEBS Lett. 579*, 3596–3600.

(29) Chan, D. C., Chutkowski, C. T., and Kim, P. S. (1998) Evidence that a prominent cavity in the coiled coil of HIV type 1 gp41 is an attractive drug target. *Proc. Natl. Acad. Sci. U.S.A. 95*, 15613–15617.

(30) Liu, S., Jing, W., Cheng, B., Lu, H., Sun, J., Yan, X., Niu, J., Farmar, J., Wu, S., and Jiang, S. (2007) HIV gp41 C-terminal heptad repeat contains multifunctional domains: relation to mechanism of action of anti-HIV peptides. *J. Biol. Chem. 282*, 9612–9620.

(31) Franke, R., Hirsch, T., Overwin, H., and Eichler, J. (2007) Synthetic mimetics of the CD4 binding site of HIV-1 gp120 for the design of immunogens. *Angew. Chem., Int. Ed. 46*, 1253–1255.

(32) Robinson, J. A. (2008) β-hairpin peptidomimetics: design, structures and biological activities. *Acc. Chem. Res. 41*, 1278–1288.

(33) Lu, M., Ji, H., and Shen, S. (1999) Subdomain folding and biological activity of the core structure from human immunodeficiency virus type 1 gp41: implications for viral membrane fusion. *J. Virol. 73*, 4433–4438.

(34) Eckert, D. M., and Kim, P. S. (2001) Design of potent inhibitors of HIV-1 entry from the gp41 N-peptide region. *Proc. Natl. Acad. Sci. U.S.A. 98*, 11187–11192.

(35) Bianchi, E., Finotto, M., Ingallinella, P., Hrin, R., Carella, A. V., Hous, X. S., Schleif, W. A., and Miller, M. D. (2005) Covalent stabilization of coiled coils of the HIV gp41 N region yields extreamely potent and broad inhibitors of viral infection. *Proc. Natl. Acad. Sci. U.S.A. 102*, 12903–12908.

(36) Zwick, M. B., Saphire, E. O., and Burton, D. R. (2004) gp41: HIV's shy protein. *Nat. Med. 10*, 133–134.

(37) Walker, L. M., Phogat, S. K., Chan-Hui, P.-Y., Wagner, D., Phung, P., Goss, J. L., Wrin, T., Simek, M. D., Fling, S., Mitcham, J. L., Lehrman, J. K., Priddy, F. H., Olsen, O. A., Frey, S. M., Hammond, P. W., Kaminsky, S., Zamb, T., Moyle, M., Koff, W. C., Poignard, P., and Burton, D. R. (2009) Broad and potent neutralizing antibodies from an African donor reveal a new HIV-1 vaccine target. *Science 326*, 285–289.

BC900502Z

JOURNAL OF VIROLOGY, Aug. 2010, p. 7558–7568 Vol. 84, No. 15
0022-538X/10/$12.00 doi:10.1128/JVI.00227-10

Enhanced Exposure of Human Immunodeficiency Virus Type 1 Primary Isolate Neutralization Epitopes through Binding of CD4 Mimetic Compounds[▽]

Kazuhisa Yoshimura,[1] Shigeyoshi Harada,[1] Junji Shibata,[1] Makiko Hatada,[1] Yuko Yamada,[2] Chihiro Ochiai,[2] Hirokazu Tamamura,[2] and Shuzo Matsushita[1]*

Division of Clinical Retrovirology and Infectious Diseases, Center for AIDS Research, Kumamoto University, Kumamoto, Japan,[1] and Institute of Biomaterials and Bioengineering, Tokyo Medical and Dental University, Chiyoda-ku, Tokyo, Japan[2]

Received 17 March 2010/Accepted 13 May 2010

***N*-(4-Chlorophenyl)-*N'*-(2,2,6,6-tetramethyl-piperidin-4-yl)-oxalamide (NBD-556) is a low-molecular-weight compound that reportedly blocks the interaction between human immunodeficiency virus type 1 (HIV-1) gp120 and its receptor CD4. We investigated whether the enhancement of binding of anti-gp120 monoclonal antibodies (MAbs) toward envelope (Env) protein with NBD-556 are similar to those of soluble CD4 (sCD4) by comparing the binding profiles of the individual MAbs to Env-expressing cell surfaces. In flow cytometric analyses, the binding profiles of anti-CD4-induced epitope (CD4i) MAbs toward NBD-556-pretreated Env-expressing cell surfaces were similar to the binding profiles toward sCD4-pretreated cell surfaces. To investigate the binding position of NBD-556 on gp120, we induced HIV-1 variants that were resistant to NBD-556 and sCD4 *in vitro*. At passage 21 in the presence of 50 μM NBD-556, two amino acid substitutions (S375N in C3 and A433T in C4) were identified. On the other hand, in the selection with sCD4, seven mutations (E211G, P212L, V255E, N280K, S375N, G380R, and G431E) appeared during the passages. The profiles of the mutations after the selections with NBD-556 and sCD4 were very similar in their three-dimensional positions. Moreover, combinations of NBD-556 with anti-gp120 MAbs showed highly synergistic interactions against HIV-1. We further found that after enhancing the neutralizing activity by adding NBD-556, the contemporaneous virus became highly sensitive to antibodies in the patient's plasma. These findings suggest that small compounds such as NBDs may enhance the neutralizing activities of CD4i and anti-V3 antibodies *in vivo*.**

Human immunodeficiency virus type 1 (HIV-1) replicates continuously in the face of a strong antibody (Ab) response, although Abs effectively control many viral infections (3). Neutralizing Abs (NAbs) are directed against the HIV-1 envelope (Env) protein, which is a heterodimer comprising an extensively glycosylated CD4-binding subunit (gp120) and an associated transmembrane protein (gp41). Env proteins are present on the virion surface as "spikes" composed of trimers of three gp120-gp41 complexes (20, 21, 29). These spikes resist neutralization through epitope occlusion within the oligomer, extensive glycosylation, extension of variable loops from the surface of the complex, and steric and conformational blocking of receptor binding sites (16, 18, 20).

Ab access to conserved regions is further limited because viral entry is a stepwise process involving conformational changes that lead to only transient exposure of conserved domains such as the coreceptor binding site (4, 5). However, some early strains of HIV-1 appear to be highly susceptible to neutralization by Abs (1, 10). For instance, subtype A HIV-1 envelopes from the early stage of infection exhibit a broad range of neutralization sensitivities to both autologous and heterologous plasma (1), suggesting that at least a subset of the envelopes have some preserved and/or exposed neutralization epitopes. It is well known that the potential for neutralizing properties of particular Abs is enhanced after binding of soluble CD4 (sCD4), especially NAbs against CD4-induced epitopes (CD4i Abs) (27) and some anti-V3 Abs (22). CD4i Abs are detected in plasma samples from many patients at an early stage of HIV-1 infection (9). Consequently, we hypothesize that small compounds such as sCD4 can enhance the neutralizing activities of CD4i Abs and some anti-V3 Abs not only *in vitro* but also *in vivo*.

In a previous report, two low-molecular-weight compounds that presumably interfere with viral entry of HIV-1 into cells were described (35). These two *N*-phenyl-*N'*-(2,2,6,6-tetramethyl-piperidin-4-yl)-oxalamide analogs, NBD-556 and NBD-557, comprise a novel class of HIV-1 entry inhibitors that block the interaction between gp120 and CD4. These compounds were found to be equally potent inhibitors of both X4 and R5 viruses in CXCR4- and CCR5-expressing cell lines, respectively (35). Schön et al. (25) also reported that NBD-556 binds to gp120 in a process characterized by a large favorable change in enthalpy that is partially compensated for by a large unfavorable entropy change, representing a thermodynamic signature similar to that observed for binding of sCD4 to gp120. In a recent study, Madani et al. (23) reported the following findings: (i) NBD-556 binds within the Phe43 cavity, a highly conserved and functionally important pocket formed as gp120 assumes the CD4-bound conformation; (ii) the NBD-556 phenyl ring projects into the Phe43 cavity; (iii) the enhancement of CD4-independent infection by NBD-556 requires the induction of conformational changes in gp120; and (iv) increased

* Corresponding author. Mailing address: Division of Clinical Retrovirology and Infectious Diseases, Center for AIDS Research, Kumamoto University, Kumamoto 860-0811, Japan. Phone: 81-96-373-6536. Fax: 81-96-373-6537. E-mail: shuzo@kumamoto-u.ac.jp.

▽ Published ahead of print on 26 May 2010.

affinities of NBD-556 analogs toward gp120 improve the antiviral potency during infection of CD4-expressing cells. The latter two studies demonstrated that low-molecular-weight compounds such as NBDs can induce conformational changes in the HIV-1 gp120 glycoprotein similar to those observed upon sCD4 binding (23, 25). The authors of these studies concluded that their data supported the importance of gp120 residues near the Phe43 cavity in binding to NBD-556 and lent credence to the docked binding mode.

In the present study, we investigated the binding position of NBD-556 on gp120 by inducing HIV-1 variants that were resistant to NBD-556 by exposing HIV-1_{IIIB} to increasing concentrations of the compound *in vitro*. We also induced sCD4-resistant HIV-1_{IIIB} variants and compared the profile of the sCD4-resistant mutations to that of the NBD-556-resistant mutations. We subsequently examined the virological properties of pseudotyped HIV-1 clones carrying the NBD-556 and sCD4 resistance-associated *env* gene mutations. Our findings provide a foundation for understanding the interaction of NBD-556 with the CD4-binding site of HIV-1 gp120. We also evaluated the anti-HIV-1 interactions between plasma NAbs and NBD-556 *in vitro* and considered the possibility of using the data as a key to opening the shield covering the conserved epitopes targeted by NAbs.

(This study was presented in part at the 15th Conference on Retroviruses and Opportunistic Infection, Boston, MA, 3 to 6 February 2008 [Abstract 736].)

MATERIALS AND METHODS

Cells, culture conditions, and reagents. The CD4-positive T-cell line PM1 was maintained in RPMI 1640 (Sigma, St. Louis, MO) supplemented with 10% heat-inactivated fetal calf serum (FCS; HyClone Laboratories, Logan, UT), 50 U of penicillin/ml, and 50 μg of streptomycin/ml. PM1/CCR5 cells were generated by standard retrovirus-mediated transduction of PM1 cells with pBABE-CCR5 provided by the National Institutes of Health AIDS Research and Preference Reagent Program (NIH ARRRP) (24, 34). PM1/CCR5 cells were maintained in RPMI 1640 supplemented with 10% heat-inactivated FCS, 50 U of penicillin/ml, 50 μg of streptomycin/ml, and 0.1 mg of G418 (Invitrogen, Carlsbad, CA)/ml. The TZM-bl cell line was obtained from the NIH ARRRP and maintained in Dulbecco modified Eagle medium (Sigma) supplemented with 10% FCS.

NBD-556 (molecular weight, 337.84) and YYA-004 (molecular weight, 303.4), which has the same structure as JRC-I-300 (23), were synthesized as previously described (23, 25, 30). KD-247 (12), 3E4, and 0.5γ (unpublished) are anti-gp120-V3 monoclonal Abs (MAbs). 17b (27), 4C11, and 4E9C (unpublished) are MAbs against CD4-induced epitopes (CD4i Abs). 17b, 2G12 (a MAb against the gp120 glycan), and b12 (a MAb against the CD4-binding site [CD4bs] epitope) were provided by the NIH ARRRP. The 0.5δ antibody established in our laboratory is an anti-CD4bs MAb (unpublished results). RPA-T4 (an anti-CD4 MAb) was purchased from BD Biosciences Pharmingen (San Jose, CA). Recombinant human sCD4 was purchased from R&D Systems, Inc. (Minneapolis, MN).

MAbs 3E4, 0.5γ, 0.5δ, 4C11, and 4E9C were human MAbs established from a patient with long-term nonprogressive illness. B cells from the patient's peripheral blood mononuclear cells (PBMC) were transformed by Epstein-Barr virus, followed by cloning. Culture supernatant from an individual clone was screened for reactivity to $gp120_{SF2}$ by enzyme-linked immunosorbent assay (ELISA). The specificity of the antibodies was determined by gp120 capture ELISA and fluorescence-activated cell sorting analysis of HIV-1_{JR-FL}-infected PM1 cells in the presence or absence of sCD4. The binding specificity was further assessed by an ELISA using peptides corresponding to the V3 sequence of various isolates. Based on these binding data, we classified them as follows: V3 MAbs, 3E4 and 0.5γ; CD4bs MAb, 0.5δ; and CD4i MAbs, 4C11 and 4E9C.

The laboratory-adapted HIV-1 strains HIV-$1_{89.6}$, HIV-1_{BaL}, HIV-1_{SF162}, HIV-1_{JR-FL}, and HIV-1_{YU2} were propagated in phytohemagglutinin-activated PBMC. These viruses were then passaged in PM1/CCR5 cells, and the culture supernatants were stored at −150°C prior to use. R5 primary HIV-1 isolates (HIV-$1_{Pt.1}$, HIV-$1_{Pt.2}$, HIV-$1_{Pt.3}$, and HIV-$1_{Pt.4}$) were isolated from four Japanese patients in our laboratory. All patients were at a stage of chronic infection. HIV-$1_{Pt.1}$, HIV-$1_{Pt.3}$, and HIV-$1_{Pt.4}$ were isolated from drug-naive patients, and HIV-$1_{Pt.2}$ was isolated from a drug-experienced patient and passaged in phytohemagglutinin-activated PBMC. Infected PBMC were cocultured with PM1/CCR5 cells for 4 to 5 days, and the culture supernatants were stored at −150°C until used. Nucleotide sequences of the gp120 from the four primary isolates were deposited in the DNA Data Bank of Japan under accession numbers AB553911 to AB553914.

Susceptibility assay. The sensitivities of six laboratory-adapted viruses, four primary isolates, and HIV-1_{IIIB} viruses passaged in the presence of sCD4 or NBD-556 were determined by the MTT [3-(4,5-dimethylthiazol-2-yl)-2,5-diphenyltetrazolium bromide] assay as previously described with minor modifications (31). Briefly, PM1/CCR5 cells (2×10^3 cells/well) were exposed to 100 times the 50% tissue culture infective dose ($TCID_{50}$) of the viruses in the presence of various concentrations of sCD4 or NBD-556 in 96-well round-bottom microculture plates, followed by incubation at 37°C for 7 days. After removal of 100 μl of the medium, 10 μl of MTT solution (7.5 mg/ml) in phosphate-buffered saline (PBS) was added to each well. The plate was then incubated at 37°C for 3 h. Subsequently, the produced formazan crystals were dissolved by adding 100 μl of acidified isopropanol containing 4% (vol/vol) Triton X-100 to each well. The optical densities at a wavelength of 570 nm were measured in a microplate reader. All assays were performed in duplicate or triplicate. We also determined the concentration for 50% cytotoxicity (CC_{50}) by using the MTT assay.

The sensitivities of the HIV-$1_{Pt.3}$ primary isolate to KD-247 (anti-V3 MAb), 4E9C (CD4i MAb), and autologous plasma IgG in the presence or absence of NBD-556 were also determined by using the MTT assay. To exclude any influence of plasma factors, such as antiviral drugs, cytokines, and chemokines, on the neutralization activities, we used IgG from the patient's plasma, which was purified using protein A-Sepharose (Affi-gel Protein A; Bio-Rad, Hercules, CA) (19).

Flow cytometric analysis. HIV-1_{JR-FL} chronically infected PM1 cells were preincubated with or without sCD4 (0.5 μg/ml) and NBD-556 (1, 3, 10, 30, 90, and 100 μM) for 15 min and then incubated with various anti-HIV-1 MAbs (17b, 4C11, KD-247, 3E4, and 0.5γ) at 4°C for 30 min. The cells were washed with PBS, and a fluorescein isothiocyanate-conjugated goat anti-human IgG Ab was used for Ab detection. Flow cytometry was performed with a FACSCalibur flow cytometer (BD Biosciences), and the data were analyzed by using the BD CellQuest version 3.1 software (BD Biosciences).

Data analysis and evaluation of synergy. Analyses of the synergistic, additive, and antagonistic effects of the antiviral agents were initially performed according to the median effect principle using the CalcuSyn version 2 computer program (6) to provide estimates of the 50% inhibitory concentration (IC_{50}) values of the antiviral agents in combination. Combination indices (CIs) were estimated from the data and reflected the nature of the interactions between KD-247 and sCD4 or NBD-556 and between NBD-556 and CD4i MAb 4C11 or anti-CD4bs MAb 0.5δ against HIV-1_{JR-FL} or HIV-1_{IIIB} on PM1/CCR5 cells as determined by the MTT assay. A CI of <0.9 indicated synergy, a CI between 0.9 and 1.1 indicated additivity, and a CI of >1.1 indicated antagonism. The CI value was directly proportional to the amount of synergy for the combination regimen. For example, values of <0.5 represented a high degree of synergy, while values of >1.5 represented significant antagonism. This approach has been widely used in analyses of antiviral interactions and was chosen to allow comparability with published literature.

Docking simulation. The structure for NBD-556 was built in SYBYL 7.1 (Tripos, St. Louis, MO) and minimized with the MMFF94 force field and partial charges (15). Using FlexSIS through its SYBYL module, docking of NBD-556 was performed into the crystal structure of gp120 obtained from the Protein Data Bank (PDB; entry 1RZJ). The binding site was defined as residues Val255, Asp368, Glu370, Ser375, Ile424, Trp427, Val430, and Val475, including residues located within a radius of 4.4 Å. The structure of the ligand was treated flexibly, and all other options were set to their default values. Figures were generated using SwissPdb Viewer version 3.9 (SPdbViewer) (13) and ViewerLite version 5.0 (Accelrys, Inc., San Diego, CA). We also generated a simian immunodeficiency virus (SIV) gp120 figure (PDB entry 2BF1) to compare the sites of the mutations in HIV-1 gp120 using the same software programs.

Isolation of NBD-556- and sCD4-resistant mutants from HIV-1_{IIIB} *in vitro*. To select NBD-556 and sCD4 escape viruses, HIV-1_{IIIB} was treated with various concentrations of NBD-556 or sCD4 and then infected into PM1/CCR5 cells as previously described with minor modifications (32). Viral replication was monitored by observation of any cytopathic effects in PM1/CCR5 cells. The culture supernatants were harvested on day 7 and used to infect fresh PM1/

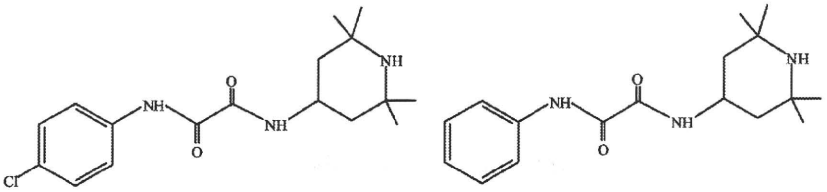

NBD-556 **YYA-004**

FIG. 1. Structures of NBD-556 and YYA-004.

CCR5 cells for the next round of culture in the presence of increasing concentrations of NBD-556 or sCD4. When the viruses began to propagate in the presence of NBD-556 or sCD4, the concentration was further increased. After the viruses were passaged using up to 50 μM NBD-556 or 20 μg of sCD4/ml in PM1/CCR5 cells, the resulting viruses, designated NBD-556(20)14p, NBD-556(50)17p, and sCD4(20)5p, were recovered from the passaged cell culture supernatants.

Proviral DNA extracts from cells cultured with several concentrations of NBD-556 and sCD4 were subjected to PCR amplification using *Taq* polymerase (Takara, Shiga, Japan). The amplified products were cloned into pCR2.1 (Invitrogen), and the *env* regions in both the passaged and selected viruses were sequenced by using an ABI Prism 3110 automated DNA sequencer (ABI, Foster City, CA).

Construction of mutant Env expression vectors. Proviral DNA was extracted from the passaged HIV-1_{IIIB}-infected PM1/CCR5 cells by using a QIAamp DNA blood minikit (Qiagen, Valencia, CA). For the construction of Env expression vectors, we used pCXN2, which contains a chicken actin promoter. Briefly, we amplified the passaged HIV-1_{IIIB} gp160 regions using LA *Taq* (Takara) with the primers ENVA (5′-GGCTTAGGCATCTCCTATGGCAGGAAGAA-3′) and ENVN (5′-CTGCCAATCAGGGAAGTAGCCTTGTGT-3′). The PCR products were inserted into pCR-XL-TOPO (Invitrogen). The EcoRI fragment of pCR-XL-IIIB containing the entire *env* region was ligated into pCXN2 to give pCXN-IIIBwt. pCXN-IIIB(S375N), pCXN-IIIB(V255E), and pCXN-IIIB(A433T) were generated by site-directed mutagenesis using a QuikChange site-directed mutagenesis kit (Stratagene, La Jolla, CA) in accordance with the manufacturer's instructions with the primer pairs S375Nfw (5′-AAATTGTAAC GCACAATTTTAATTGTGGAGG-3′) and S375Nrv (5′-CCTCCACAATTAA AATTGTGCGTTACAATTT-3′), V255Efw (5′-GAATTAGGCCAGTAGAAT CAACTCAACTGCT-3′) and V255Erv (5′-AGCAGTTGAGTTGATTCTACT GGCCTAATTC-3′), and A433Tfw (5′-CAGGAAGTAGGAAAAACAATGTA TGCCCCTC-3′) and A433Trv (5′-GAGGGGCATACATTGTTTTTCCTACTT CCTG-3′), respectively.

Pseudovirus preparation. Portions, 5 μg of pSG3ΔEnv and 0.5 μg of pRSV-Rev (17), supplied by the NIH ARRRP, and a 4.5-μg portion of HIV-1_{IIIB} Env-expressing pCXN2 were cotransfected into 293T cells using the Effectene transfection reagent (Qiagen). At 48 h after transfection, the pseudovirus-containing supernatants were harvested, filtered through a 0.2-μm-pore-size filter, and stored at −80°C. The pseudovirus activities were measured with a luminescence assay using TZM-bl cells as previously described (28).

Single-round virus infection assay. A single-cycle infectivity assay was used to measure the neutralization of HIV-1_{IIIB} pseudoviruses as described previously (26, 28). Briefly, NBD-556, YYA-004, sCD4, 2G12, b12, RPA-T4, or 4C11 at various concentrations and a pseudovirus suspension corresponding to 100 $TCID_{50}$ were preincubated in the absence or presence of 1 μM NBD-556 for 15 min on ice. The virus-compound mixtures were added to TZM-bl cells, which had been seeded in a 96-well plate (1.5×10^4 cells/well) on the previous day. The cultures were incubated for 2 days at 37°C, washed with PBS, and lysed with lysis solution (Galacto-Star mammalian reporter gene assay system; ABI). After transfer of the cell lysates to luminometer plates, the β-galactosidase activity (in relative light units) in each well was measured by using 50-fold-diluted Galacto-Star substrate in a reaction buffer diluent (100 μl/well; ABI) in a TR717 microplate luminometer (ABI). The reduction in infectivity was determined by comparing the relative light units in the presence or absence of each compound and expressed as the percentage of neutralization. Each assay was repeated two to three times.

RESULTS

Anti-HIV-1 activities of sCD4, NBD-556, and YYA-004 for laboratory strains and primary HIV-1 isolates. Initially, we determined the inhibitory activities of sCD4, NBD-556, and YYA-004, which has a phenyl group instead of the *p*-chlorophenyl group of NBD-556 (Fig. 1), on the infection of PM1/CCR5 cells by different laboratory-adapted HIV-1 strains and different HIV-1 primary isolates of subtype B, including both X4 and R5 viruses, by using a previously reported method (33). sCD4 inhibited the laboratory-adapted HIV-1 strains HIV-1_{IIIB}, HIV-$1_{89.6}$, HIV-1_{BaL}, HIV-1_{SF162}, HIV-1_{JR-FL}, and HIV-1_{YU2} with IC_{50}s ranging from 0.26 to 6.1 μg/ml (Table 1). NBD-556 inhibited the X4 virus HIV-1_{IIIB} and dualtropic virus HIV-$1_{89.6}$ with IC_{50}s of 7.8 and 11.4 μM, respectively, but did not inhibit the R5 viruses HIV-1_{BaL}, HIV-1_{SF162}, HIV-1_{JR-FL}, and HIV-1_{YU2} with IC_{50}s of >30 μM. We also tested sCD4 and NBD-556 against the R5 primary isolates HIV-$1_{Pt.1}$, HIV-$1_{Pt.2}$, HIV-$1_{Pt.3}$, and HIV-$1_{Pt.4}$. sCD4 effectively inhibited all of the primary isolates at concentrations of 0.2 to 7.4 μg/ml. On the other hand, NBD-556 inhibited two of the four primary

TABLE 1. Inhibitory activities of sCD4 and NBD-556 toward infection by laboratory and primary strains of HIV-1

Virus	Subtype	Cell	Mean IC_{50}[a] ± SD		
			sCD4 (μg/ml)	NBD-556 (μM)	YYA-004 (μM)
Laboratory-adapted viruses					
X4					
HIV-1_{IIIB}	B	PM1/CCR5	0.26 ± 0.17	7.8 ± 2.6	>100
Dual					
HIV-$1_{89.6}$	B	PM1/CCR5	0.87 ± 0.09	11.4 ± 2.4	>100
R5					
HIV-1_{BaL}	B	PM1/CCR5	1.7 ± 0.28	>30	>100
HIV-1_{SF162}	B	PM1/CCR5	3.6 ± 0.64	>30	>100
HIV-1_{JR-FL}	B	PM1/CCR5	3.6 ± 0.71	>30	>100
HIV-1_{YU2}	B	PM1/CCR5	6.1 ± 2.00	>30	>100
Primary isolates					
R5					
HIV-$1_{Pt.1}$	B	PM1/CCR5	0.2 ± 0.04	3.6 ± 0.67	>100
HIV-$1_{Pt.2}$	B	PM1/CCR5	1.6 ± 0.21	>30	>100
HIV-$1_{Pt.3}$	B	PM1/CCR5	3.7 ± 0.42	11.8 ± 1.6	>100
HIV-$1_{Pt.4}$	B	PM1/CCR5	7.4 ± 1.30	>30	>100

[a] PM1/CCR5 cells (2×10^3) were exposed to 100 $TCID_{50}$ of each virus and then cultured in the presence of various concentrations of sCD4, NBD-556, or YYA-004 as indicated. The IC_{50}s were determined by using the MTT assay on day 7 of culture. All assays were conducted in duplicate, and the data shown represent the means derived from the results of two to three independent experiments. For NBD-556, CC_{50} = 140 μM; for YYA-004, CC_{50} = 350 μM. (The CC_{50} is the concentration for 50% cytotoxicity.)

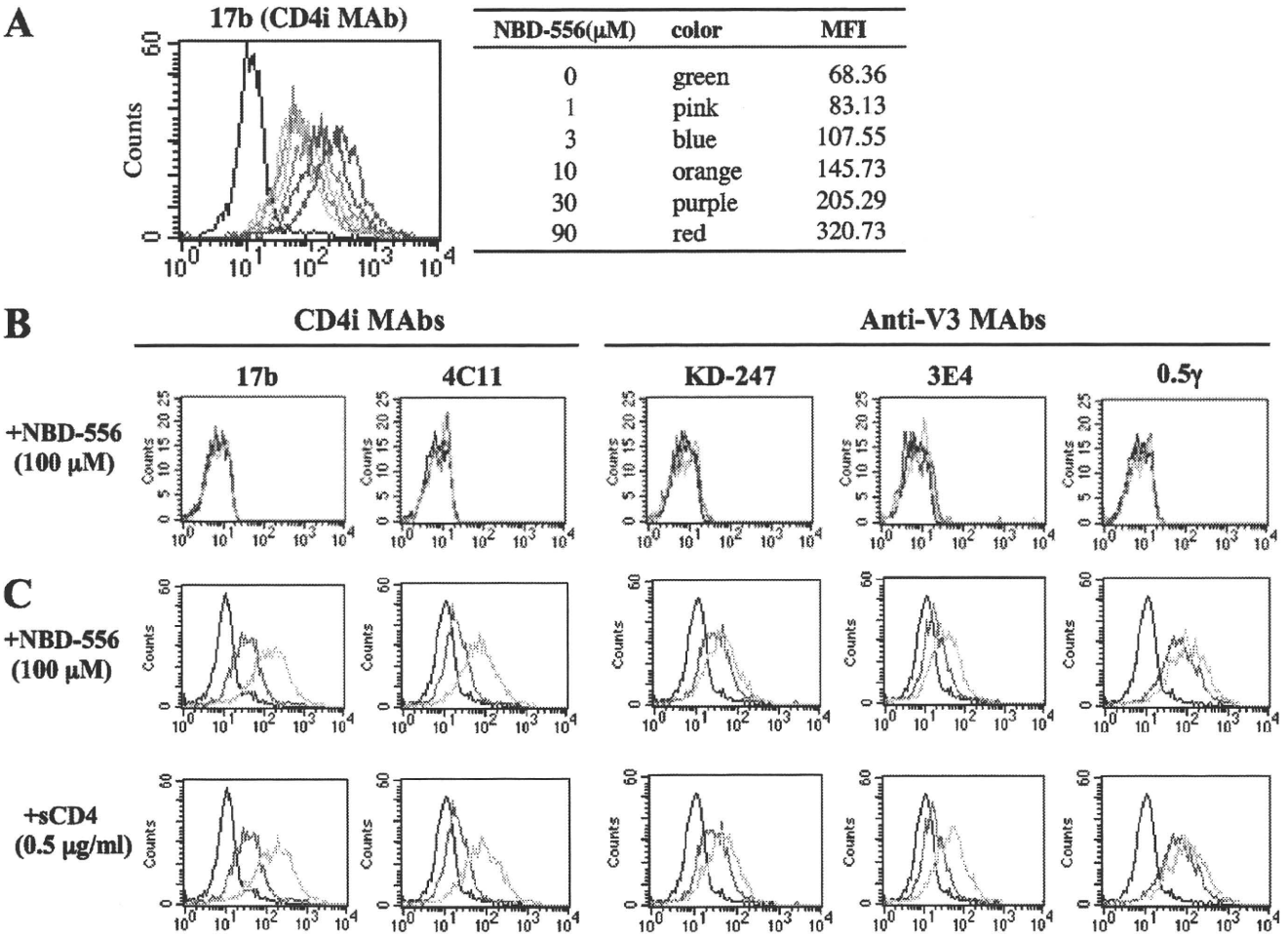

NBD-556(μM)	color	MFI
0	green	68.36
1	pink	83.13
3	blue	107.55
10	orange	145.73
30	purple	205.29
90	red	320.73

FIG. 2. Comparisons of MAb binding to cell surface-expressed gp120 with sCD4 and NBD-556. HIV-1_{JR-FL} chronically infected PM1 cells were preincubated with or without NBD-556 (A, 1 to 90 μM; C, 100 μM) or sCD4 (C, 0.5 μg/ml), and uninfected PM1 cells were also preincubated with or without NBD-556 (B, 100 μM) for 15 min, and then incubated with various anti-HIV-1 MAbs (17b, 4C11, KD-247, 3E4, and 0.5γ) at 4°C for 30 min. The cells were washed, and a fluorescein isothiocyanate-conjugated anti-human IgG was used for detection. (A) Color lines show the concentrations of NBD-556: green, 0 μM; pink, 1 μM; blue, 3 μM; orange, 10 μM; purple, 30 μM; and red, 90 μM. (B and C) Red line shows no preincubated with NBD-556 or sCD4. Blue line shows preincubated with NBD-556 or sCD4. Black line shows using a control IgG MAb.

isolates, HIV-$1_{Pt.1}$ and HIV-$1_{Pt.3}$, with IC_{50}s of 3.6 and 11.8 μM, respectively (Table 1). YYA-004 did not show significant anti-HIV activity against any of the strains tested up to a concentration of 100 μM. The *in vitro* cytotoxicities of NBD-556 and YYA-004 toward PM1/CCR5 cells used for the anti-HIV-1 infectivity studies were determined by using the MTT assay. The CC_{50} values of NBD-556 and YYA-004 toward PM1/CCR5 cells were 140 and 350 μM, respectively (Table 1).

Comparison of Ab binding to cell surface-expressed HIV-1_{JR-FL} Env with NBD-556 and sCD4. To compare the effect of NBD-556 with that of sCD4 with respect to the induction of conformational change in the trimeric gp120, the binding of CD4i MAbs (17b and 4C11) and anti-V3 MAbs (KD-247, 3E4, and 0.5γ) to cell surface-expressed Env proteins on HIV-1_{JR-FL} chronically infected PM1 cells was analyzed by fluorescence-activated cell sorting. Comparisons of the binding profiles of the Abs to the cell surfaces were carried out using the mean fluorescence intensity (MFI). The binding of CD4i MAb 17b increased gradually as the amount of the CD4-mimicking small compound NBD-556 increased from 0 to 90 μM (Fig. 2A, the MFI increased from 68.36 to 320.73). As shown in Fig. 2C, the binding of both CD4i MAbs 17b and 4C11 increased remarkably after pretreatment with 100 μM NBD-556 (the MFIs increased from 43.3 to 201.57 and from 24.43 to 96.06, respectively). Moreover, the binding of all of the anti-V3 MAbs—KD-247, 3E4, and 0.5γ—was enhanced by pretreatment with NBD-556 (the MFIs increased from 34.59 to 51.9, from 22.97 to 39.07, and from 86.61 to 145.08, respectively). sCD4 pretreatment of the Env-expressing cell surface also caused remarkable enhancement of the binding for not only the CD4i MAbs but also the three anti-V3 MAbs, similar to pretreatment with NBD-556. These results indicate that the CD4-mimicking compound NBD-556 can induce the conformational changes in gp120 that are caused by binding of sCD4.

Highly synergistic interactions of KD-247 combined with NBD-556. Both neutralizing anti-V3 MAb KD-247 and NBD-556 block the viral entry process, especially at the stage of the interaction between CD4 and gp120 (CD4-binding site). Each of these agents binds to either the V3 loop or the CD4 cavity. Furthermore, our previous observations suggested that neu-

TABLE 2. Combination indices for KD-247, 4C11, or 0.5δ and for sCD4 or NBD-556 against HIV-1_{JR-FL} and HIV-1_{IIIB}

Combination	Virus	CI values at different ICs[a]		
		IC_{50}	IC_{75}	IC_{90}
KD-247+sCD4	HIV-1_{JR-FL}	0.313	0.266	0.277
KD-247+NBD-556	HIV-1_{JR-FL}	0.174	0.043	0.011
4C11+NBD-556	HIV-1_{IIIB}	0.473	0.445	0.860
0.5δ+NBD-556	HIV-1_{IIIB}	47.8	20.1	8.56

[a] The multiple-drug effect analysis of Chou et al. (6) was used to analyze the effects of the drugs in combination. IC, inhibitory concentration. CI < 0.9, synergy; CI = 0.9 to 1.1, additivity; CI > 1.1, antagonism. The data shown are representative of two or three separate experiments.

TABLE 3. Inhibitory activities of NBD-556 and sCD4 toward infection of HIV-1_{IIIB} escape variants from NBD-556 and sCD4

Virus	IC_{50}[a]	
	NBD-556 (μM)	sCD4 (μg/ml)
HIV-1_{IIIB}	12	0.52
HIV-$1_{NBD-R(20)14p}$	>30	5.7
HIV-$1_{NBD-R(50)17p}$	>30	>10
HIV-$1_{sCD4-R(20)5p}$	>30	>10

[a] PM1/CCR5 cells (2×10^3) were exposed to 100 $TCID_{50}$ of each passaged virus and then cultured in the presence of various concentrations of sCD4 or NBD-556. The IC_{50}s were determined by using the MTT assay on day 7 of culture. All assays were conducted in duplicate. The data shown are representative of two or three separate experiments.

tralizing MAb KD-247 selects escape variants with greater sensitivities to sCD4 (33). Based on this notion, we examined the synergy of this MAb with sCD4 or the CD4-mimicking compound NBD-556 against wild-type HIV-1_{JR-FL}. The multiple-drug effect analysis of Chou et al. (6) was used to analyze the effects of combining KD-247 with sCD4 or NBD-556. As shown in Table 2, all of the CI values for KD-247 with the two CD4-gp120 interaction inhibitors (sCD4 and NBD-556) were <0.5 against HIV-1_{JR-FL} at all of the inhibitory concentrations tested. In particular, the CI values for the combinations of KD-247 with NBD-556 were <0.1 for IC_{75} and IC_{90}. These results suggest that combinations of KD-247 with the CD4-gp120 binding inhibitors sCD4 and NBD-556 produce very highly synergistic effects. We further examined the synergy of CD4i MAb 4C11 or anti-CD4bs MAb 0.5δ with NBD-556 against wild-type HIV-1_{IIIB}. The combination of 4C11 and NBD-556 showed synergy against HIV-1_{IIIB} for IC_{50} and IC_{75}. As expected, the IC values for NBD-556 and anti-CD4 binding site MAb, 0.5δ, which may compete with the CD4 mimetic for the CD4-binding site, were >5 against HIV-1_{IIIB} at all of the inhibitory concentrations tested. However, at lower concentrations, additive effects were observed between NBD-556 and anti-CD4bs MAb 0.5δ (data not shown). These results indicate that NBD-556 may bind within or near the epitope of the anti-CD4bs MAb and then induce the conformational changes in Env.

Selection of NBD-556 and sCD4 escape variants. To select NBD-556- and sCD4-resistant HIV-1 variants *in vitro*, we exposed PM1/CCR5 cells to HIV-1_{IIIB} and serially passaged the viruses in the presence of increasing concentrations of NBD-556 or sCD4. As a control, HIV-1_{IIIB} was passaged under the same conditions without the antiviral agents to allow us to monitor the spontaneous changes that occurred in the virus during prolonged PM1/CCR5 cell passages (designated the passage control). The selected viruses were initially propagated in the presence of 1 μM NBD-556 or 0.5 μg of sCD4/ml and, during the course of the selection procedure, the concentrations of the NBD-556 and sCD4 were increased to 50 μM and 20 μg/ml, respectively. At passages 14 and 17 for NBD-556 and passage 5 for sCD4, the supernatants containing the viruses, which were designated HIV-$1_{NBD-R(20)14p}$, HIV-$1_{NBD-R(50)17p}$, and HIV-$1_{sCD4-R(20)5p}$, respectively, were harvested, and the sensitivities of the viruses to NBD-556 and sCD4 were determined by the MTT assay (Table 3). The IC_{50}s for NBD-556 against HIV-1_{IIIB}, HIV-$1_{NBD-R(20)14p}$, and HIV-$1_{NBD-R(50)17p}$ were 12, >30, and >30 μM, respectively. The IC_{50}s of sCD4 against HIV-1_{IIIB} and HIV-$1_{sCD4-R(20)5p}$ were 0.52 and >10 μg/ml, respectively. HIV-$1_{NBD-R(20)14p}$, HIV-$1_{NBD-R(50)17p}$, and HIV-$1_{sCD4-R(20)5p}$ were also examined for their cross-resistance with one another. Each resistant variant was found to be cross-resistant to NBD-556 and sCD4 (Table 3). These results indicate that the HIV-1_{IIIB} virus acquired resistant phenotypes against NBD-556 and sCD4 during the distinct *in vitro* selection processes.

Sequences of the envelope region of the NBD-556 and sCD4 mutants. To determine the genetic basis of the resistance in the variant HIV-1_{IIIB} strains, the C1 to C4 region of the *env* gene was amplified from genomic DNA extracted from the infected cells and cloned, and the PCR-amplified products were sequenced (Fig. 3). At passage 8 for 6 μM NBD-556, five mutations (A281D, E370A, S375N, A433T, and A436T) were observed. At passage 21 in the culture where HIV-1_{IIIB} was propagating in the presence of 50 μM NBD-556, four amino acid substitutions of Ser to Asn at position 375 (S375N, 11 of 11 clones) in C3, Ala to Lys at position 342 (A432K, 1 of 11 clones) in C4, Ala to Thr at position 433 (A433T, 4 of 11 clones) in C4, and Ala to Thr at position 436 (A436T, 1 of 11 clones) in C4 were observed (Fig. 3A). These results did not contradict a previous study in which gp120 mutants (S375W, I424A, W427A, and M475A) with changes in residues that contacted the Phe43 cavity did not detectably bind NBD-556 by isothermal titration calorimetry (23). On the other hand, in the selection with sCD4, seven mutations (E211G, P212L, V255E, N280K, S375N, G380R, and G431E) appeared during the passages. At passage 5 in the culture where HIV-1_{IIIB} was propagating in the presence of sCD4 (20 μg/ml), four substitutions of E211G (1 of 10 clones), V255E (5 of 10 clones), G380R (1 of 10 clones), and G431E (2 of 10 clones) were detected for sCD4 at 20 μg/ml (Fig. 3B).

To compare the two mutation profiles obtained during the *in vitro* selection with NBD-556 and sCD4, molecular modeling of NBD-556 docked into gp120 was performed by docking simulations using the FlexSIS module of SYBYL 7.1 (Fig. 4). The atomic coordinates of the crystal structure of gp120 with sCD4 were retrieved from the PDB (entry 1RZJ). As shown in Fig. 4, almost all of the mutations lay along the inside of the CD4 cavity in the selection of NBD-556, with similar three-dimensional positions to the mutations induced by sCD4. These findings demonstrate that NBD-556 binds to the CD4 cavity or in the vicinity of the CD4-binding site.

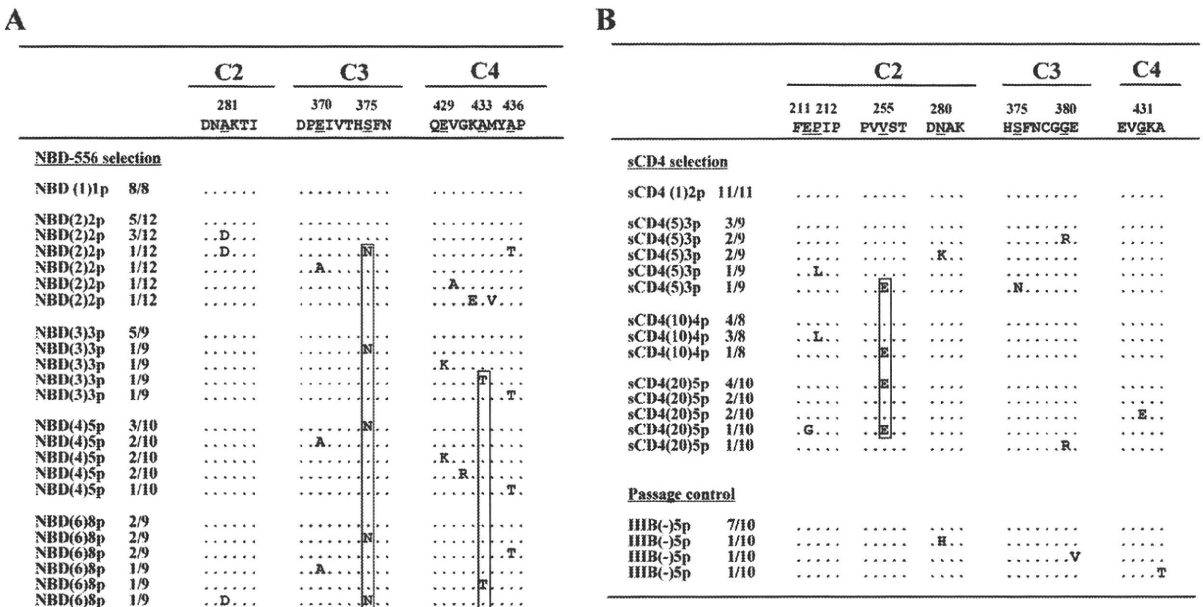

FIG. 3. Alignment of the gp120 amino acid sequences from the indicated passages in the NBD-556 and sCD4 escape processes. The amino acid sequences were deduced from the nucleotide sequences of the *env*-encoding regions of proviral DNA isolated from cells infected with the HIV-1_{IIIB} variants selected in the presence of NBD-556 (A) or sCD4 (B) and the passage control. The amino acid sequences of the envelope proteins of the baseline HIV-1_{IIIB} are shown at the top as a reference. The identity of the sequences at the individual amino acid positions is indicated by dots. The numbers of clones with the given amino acid substitutions among a total of 8 to 12 clones are listed. The number in parentheses denotes the concentrations of NBD-556 or sCD4. The major mutations of NBD-556 and sCD4-resistant variants at final passage are boxed.

Sensitivities of β-galactosidase reporter HIV strains pseudotyped with the sCD4- and NBD-556-resistant envelope mutations to NBD-556, sCD4, and MAbs. To confirm whether the mutations were responsible for the reduced sensitivities to NBD-556 and sCD4, a single-round replication assay was performed. The β-galactosidase reporter viruses were pseudotyped with wild-type Env (HIV-1_{WT}) or Env singly mutated with V255E in C2 (HIV-1_{V255E}), S375N in C3 (HIV-1_{S375N}), and A433T in C4 (HIV-1_{A433T}). The mutations that arose in the absence of NBD-556 (the passage control) are not related to resistance because the control passage did not show any significant increase in IC_{50} (data not shown). With respect to the mutations in the presence of NBD-556 three mutations, S375N, V255E, and A433T were consistently and increasingly observed during the process of selection. Additional mutations in "escape variants" other than S375N, V255E, and A433T were observed; however, these mutations were not consistently detected in passages and did not accumulate during selection. Thus, we considered the three mutations—S375N, V255E, and A433T—related to the development of resistance to both NBD-556 and sCD4, although some involvement of additional mutations in the development of a resistant phenotype is undeniable. As shown in Fig. 5A, all of the mutant clones were completely resistant to NBD-556 at concentrations of up to 20 μM. YYA-004 without the *p*-chlorophenyl group was unable to inhibit infection of all of the clones tested (Fig. 5B). The clone with V255E, which was induced by *in vitro* selection with sCD4, was highly resistant to sCD4 compared to the wild-type virus (114-fold-higher IC_{50}) (Fig. 5C). However, the other pseudotyped viruses, HIV-1_{S375N} and HIV-1_{A433T}, were slightly resistant compared to HIV-1_{WT} (4- and 2-fold-higher IC_{50}s, respectively). We also examined the sensitivities of the pseudotyped clones containing Env mutations to anti-gp120 glycan MAb 2G12, anti-CD4bs MAb b12, and anti-CD4 MAb RPA-T4 by a single-round replication assay (Fig. 5D to F). All of the mutant viruses showed almost the same neutralization sensitivities as the wild-type virus to the 2G12, b12, and RPA-T4 MAbs. These results indicate that the three mutations induced by *in vitro* selection with NBD-556 and sCD4 were responsible for the resistance to NBD-556, whereas the NBD-selected variants containing S375N in C3 and A433T in C4 of gp120 had moderately resistant phenotypes against sCD4, as shown by the sensitivities of the NBD-556-passaged viruses to sCD4 determined by the multiround assay (Table 3).

To examine whether the resistance mutations affected the sensitivity of a CD4i MAb against HIV-1, we determined the